



**HAL**  
open science

# Variations of suspended particulate matter concentrations of the Mackenzie River plume (Beaufort Sea, Arctic Ocean) over the last two decades

Anastasia Tarasenko, David Doxaran, Bernard Gentili

## ► To cite this version:

Anastasia Tarasenko, David Doxaran, Bernard Gentili. Variations of suspended particulate matter concentrations of the Mackenzie River plume (Beaufort Sea, Arctic Ocean) over the last two decades. *Marine Pollution Bulletin*, 2023, 196, pp.115619. 10.1016/j.marpolbul.2023.115619 . hal-04249683

**HAL Id: hal-04249683**

<https://hal.sorbonne-universite.fr/hal-04249683v1>

Submitted on 19 Oct 2023

**HAL** is a multi-disciplinary open access archive for the deposit and dissemination of scientific research documents, whether they are published or not. The documents may come from teaching and research institutions in France or abroad, or from public or private research centers.

L'archive ouverte pluridisciplinaire **HAL**, est destinée au dépôt et à la diffusion de documents scientifiques de niveau recherche, publiés ou non, émanant des établissements d'enseignement et de recherche français ou étrangers, des laboratoires publics ou privés.



Distributed under a Creative Commons Attribution 4.0 International License

# Marine Pollution Bulletin

## Variations of suspended particulate matter concentrations of the Mackenzie River plume (Beaufort Sea, Arctic Ocean) over the last two decades

--Manuscript Draft--

<b>Manuscript Number:</b>	MPB-D-23-01850R1
<b>Article Type:</b>	Research Paper
<b>Keywords:</b>	suspended particulate matter; ocean optics; Arctic Ocean; Mackenzie; satellite data; in situ measurements
<b>Corresponding Author:</b>	Anastasia Tarasenko, PhD  FRANCE
<b>First Author:</b>	Anastasia Tarasenko, PhD
<b>Order of Authors:</b>	Anastasia Tarasenko, PhD  David Doxaran  Bernard Gentili
<b>Abstract:</b>	<p>This work addresses the last 20 years' evolution of the suspended particulate matter (SPM) concentrations in the Beaufort Sea (Canadian Arctic Ocean) directly influenced by the Mackenzie River discharge. The SPM variations in the coastal zone are highlighted and related to the freshwater and solid discharges of the river measured in situ at the Arctic Red River station (150 km upstream of the river delta). The correlation between the variations of the river discharge and SPM concentration within the surface layer of the coastal waters is obvious. Rather unexpectedly, both have been slightly but significantly decreasing from 2003 to 2018-2019 and started to increase very recently (2019-2022). This change of regime could be explained by changing patterns of precipitation (especially in winter), groundwater distribution and wind-induced mixing in the coastal area.</p>
<b>Suggested Reviewers:</b>	Jacek Andrzej Urbanski oceju@univ.gda.pl  Claireg Griffin griffin.claireg@gmail.com  Joaquín Chaves joaquin.chaves@nasa.gov

We would like to thank the reviewer for his/her work, valuable comments and suggestions. Below we answer to each of them separately.

Reviewers' comments:

“The work is another study concerning the inflow of various substances (SPM, organic carbon) into the Arctic Ocean from the Mackenzie River. Due to distinct trends in air temperature in these regions and the overall ecosystem sensitivity, this topic is of significant importance. The study encompasses recent years (up to 2022), which is crucial. The paper includes all necessary elements and is clearly written. The figures are appropriate, but authors are recommended to include:

*boxplots for SPM and annual discharge sums.”*

The annual discharge sums were indeed not indicated in text (no number were provided explicitly), but we used them for the Pearson correlation matrix (Fig. 1 in Appendix). We added the annual discharge sums to the **legend box** of Fig.1 for each year (see below).

As for the boxplots for the SPM, we would appreciate to implement it, but unfortunately, could not understand what figure was referred. In case of Fig.1d, there are too few datapoints to add the boxplots, and in case of Fig. 2(b, d, f), there is too many datapoints, as they are daily means (Fig;2.d, f).

*“My general comments are listed below.*

*The conducted reevaluation and use of new regression analysis methods provide a fresh perspective on the phenomena. However, the change in trend based on 3 years raises evident doubts and it might be worth discussing its significance further (especially considering that the only other study pertains to medical data).”*

Thank you for this comment.

We have to add that although we do not cite other works using a segmented regression analysis, the method suggested by Muggeo, 2003 was also applied to various geophysical datasets (there are about 1900 citations of this work mentioned at

[https://scholar.google.com/scholar?cites=16460629970310398020&as\\_sdt=2005&scioldt=0,5&hl=f](https://scholar.google.com/scholar?cites=16460629970310398020&as_sdt=2005&scioldt=0,5&hl=f)), e.g.:

*Zhang, S., Gan, T. Y., Bush, A. B., Liu, J., Zolina, O., & Gelfan, A. (2023). Changes of the streamflow of northern river basins of Siberia and their teleconnections to climate patterns. International Journal of Climatology.*

*Lee, E., Epstein, J. M., & Cohen, M. J. (2023). Patterns of Wetland Hydrologic Connectivity Across Coastal-Plain Wetlandscapes. Water Resources Research, e2023WR034553.*

*Börgel, F., Neumann, T., Rooze, J., Radtke, H., Barghorn, L., & Meier, H. E. (2023). Deoxygenation of the Baltic Sea during the last millennium. Frontiers in Marine Science.*

Indeed, the positive trends for the last three years are not statistically significant, and the monitoring should be continued. We discussed the significance of trends in section 3, and mentioned that the positive trends for the river discharge are not significant in paragraph #6:

“The positive trend from 2019 to the present,  $slope_{2Q} = 640.05x + const$ , **although not statistically significant**, can indicate a progressive increase in the minimum flow impacted by a “mobilization of ground waters” as discussed by Yang et al. 2015.”

And in paragraph #7 of section 3 we say that the SPM (in situ and satellite) positive trends are questionable:

“The breakpoint of  $SPM_{in situ}$  trends is slightly shifted to 2018, and CIs contain zero, thus indicating that the *segmented* model is **less reliable** for this dataset. <...>

The positive trends  $slope_{2sat}$  and  $slope_{2sat200}$  **are not statistically significant**, and their SEs are of the order of the estimated coefficient of linear regression (Tab.1). Nevertheless, this result is interesting for further discussion”

We added in the last paragraph of the conclusion an additional indication about statistical significance of the positive trend.

*I also have reservations about the presentation of the hypothetical mechanism explaining the observed negative trend in river discharge and SPM concentration, which suddenly switches to a rapid positive trend. Since this is an original aspect of the study, the discussion should be supported by literature describing the mentioned mechanisms.*

Thank you for this comment. We discussed the results with our colleagues hydrologists, and indeed changed the optics for the possible explanation of observed trends. Please, see the last three paragraphs of the results and discussion section, together with the updated Conclusions section.

*The authors should include a discussion on the dynamics of the coastal zone. For instance, storms could influence the determined concentrations in the coastal area. Perhaps some seasons were more dynamic, while others were less so?*

Thank you for this suggestion, we added to the analysis the wind data from ERA5 (marine area similar to that chosen for the MODIS study box).

The hypothesis that the wind stress will induce the vertical mixing and affect the SPM concentration in water is clear and reasonable. Nevertheless, there is one fundamental limitation for this analysis due to the nature of ocean color data retrieval from satellite: the highest wind speed (and thus mixing events) will mostly occur under the cloud cover with the passage of cyclones, and SPM concentrations cannot be retrieved from ocean color satellite under such conditions (presence of clouds).

To include the effect of storms to the Pearson correlation matrix (where the yearly parameters are compared), we included the *number of days of storms per year* as a new parameter (ndays\_storm in Fig. 1Appendix). The day was considered stormy if over the study area there was a wind vector with a wind speed over 15 m/s. The negative correlation between days of storm and cumulative annual SPM is weak (-0.19), any conclusion can hardly be done based on this result.

Then we took the *wind speed* (the absolute value of wind vector) for each moment of time, when SPM retrieved from MODIS satellite data was available, and *averaged for the whole study area* both *Uwind\_mean* and *SPM\_MODIS\_mean* (Fig. R2). The linear fit between the spatially averaged SPM and wind speed was low as well:  $y = 0.24x + 10.71$  (where  $x$  is wind speed and  $y$  is SPM concentration).

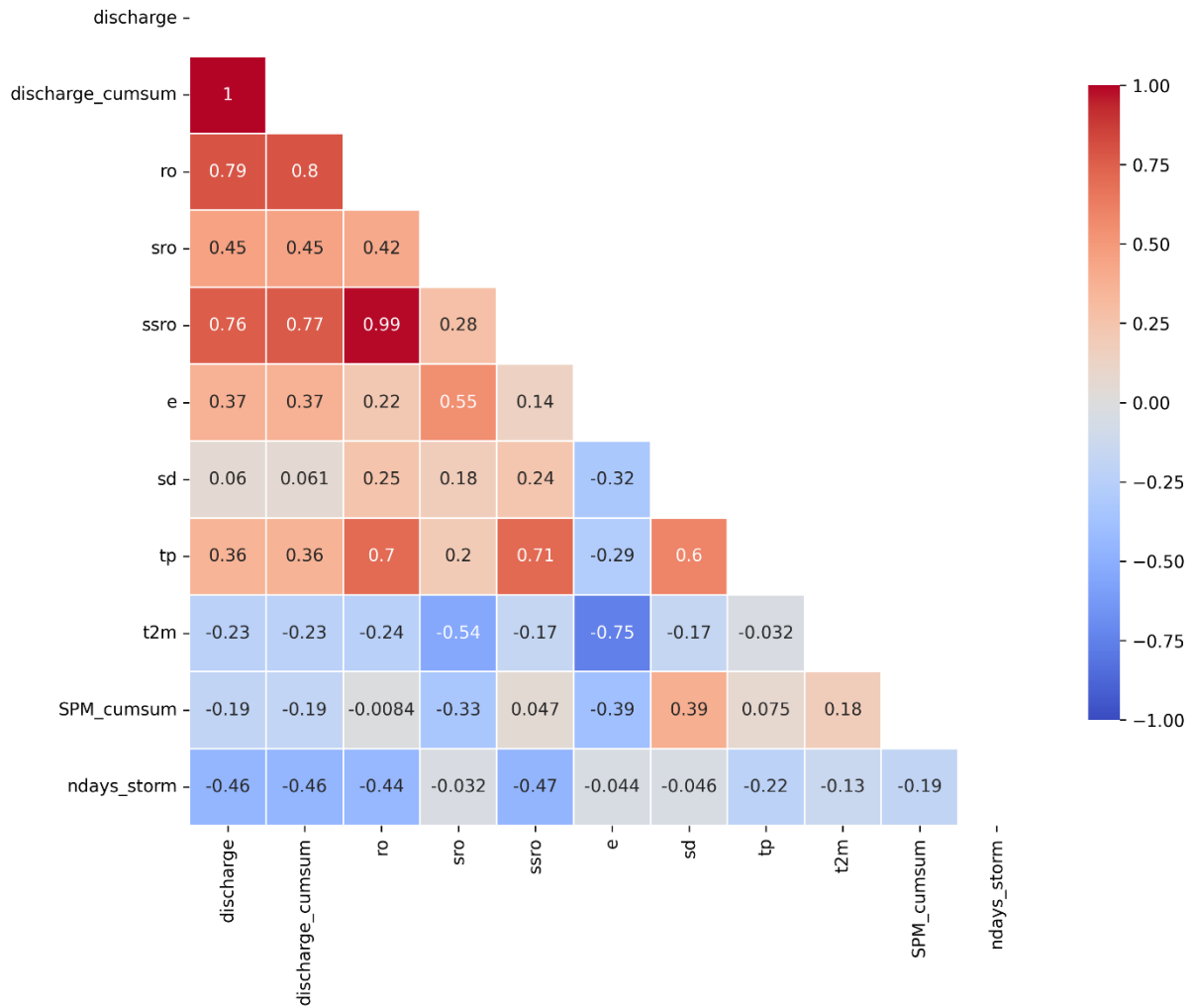


Fig.R1 Pearson correlation matrix with a new parameter referring to wind (ndays\_storm).

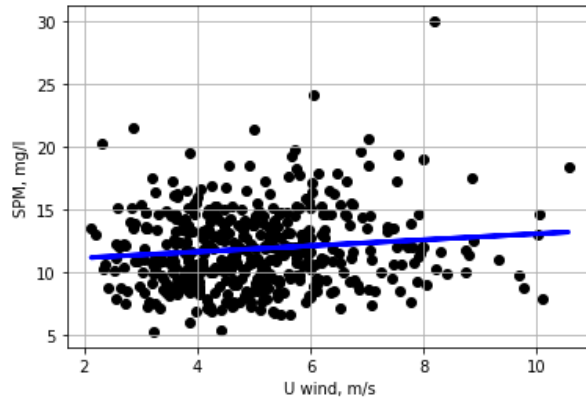
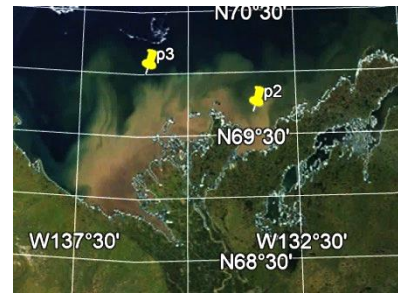


Fig.R2 Wind speed and SPM MODIS averaged over the study area for each moment of time. The blue line shows the fit

Then we tried to apply the segmented correlation method to the wind data over two sample points close to the regular river plume frontal position:  $69.7^{\circ}N, -133.5^{\circ}W$  and  $70^{\circ}N, 136W$ .



The mean wind speed force varies from 8.5 to 10.5 m/s overall, and there is no distinguishable particular pattern (Fig. R3, red line shows the linear fit).

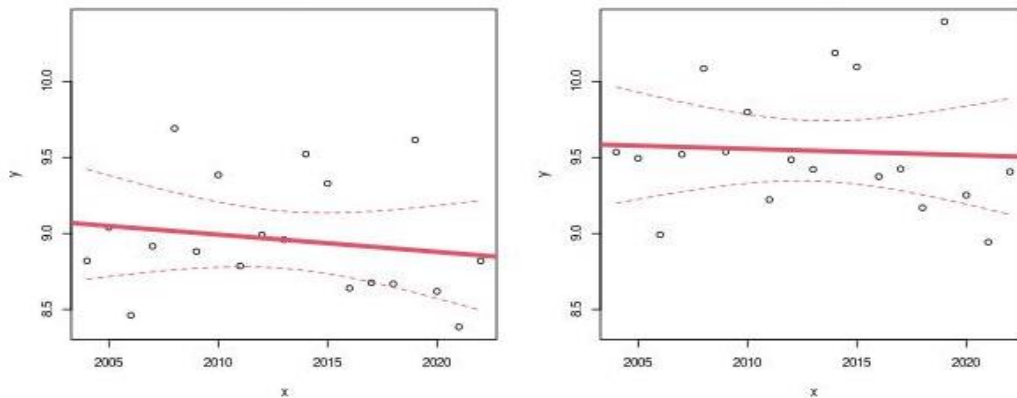


Fig. R3. Regression analysis applied to the wind force in 2 study points (left:  $69.7^{\circ}N, -133.5^{\circ}W$ , right:  $70^{\circ}N, 136W$ ). The x axis is time, y axis is wind force in m/s

The only parameter that changes slightly over the 2004-2022 period is the wind direction (Fig. R4): According to linear fits, in both points, from 2004 to  $\sim 2020$  the wind direction turned from SWW to SSW (from  $-100^{\circ}$  to  $-130^{\circ}$  from north).

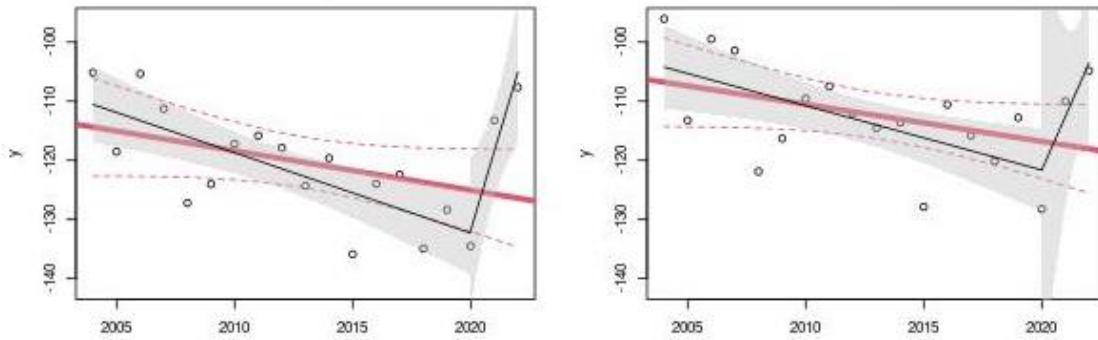


Fig. R4. Regression analysis applied to the wind direction in 2 study points (left: 69.7°N, -133.5°W, right: 70°N, 136°W). The x axis is time, y axis is wind direction in degrees from North. Red line is a linear regression result, black line is segmented regression method



Fig. R5. Illustration of possible effect of wind direction change (yellow and orange arrows), and the Ekman effect (green arrow).

This change in direction suggests rather complex consequences because of the coastal system of currents.

While the SWW wind direction (Fig.R5, left) is changing to SSW (Fig.R5; right), the Ekman effect might:

- bring the river plume into a small coastal vortex in the Mackenzie bay. In this case the SPM has more chances to recirculate within the delta area (higher SPM concentration?), but also be sedimented on the floor (lower SPM concentration)
- bring the SPM further offshore into the westward or eastward system of currents. In both cases, the SPM concentration reduces.

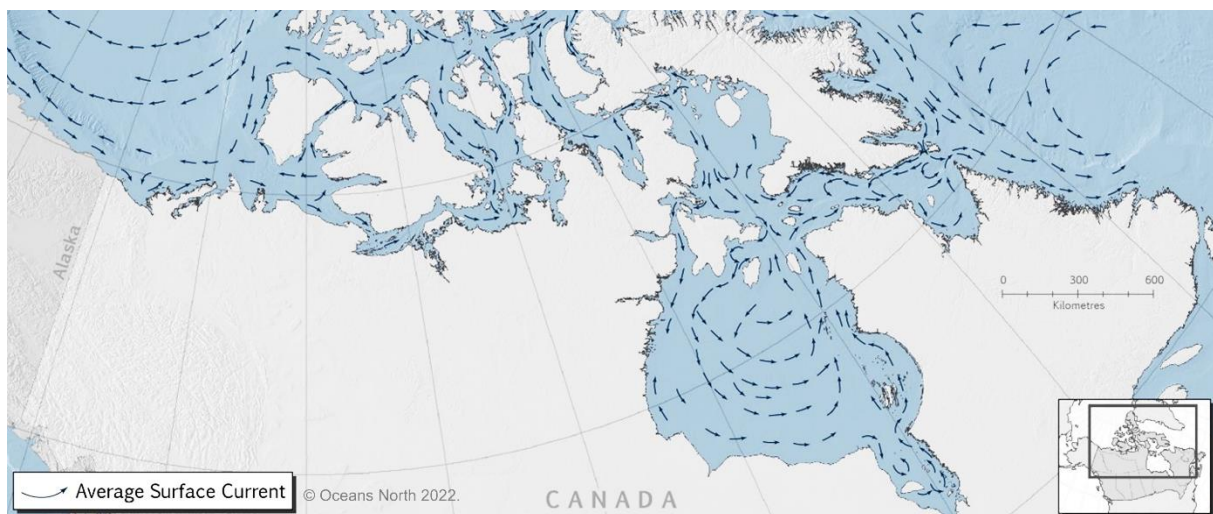


Fig. R6. Surface currents in Canadian Arctic basin (from <https://www.oceansnorth.org/wp-content/uploads/2018/07/en-02-canadas-arctic-marine-atlas-chapter-two-physical-oceanography.pdf>)

After this analysis, we conclude that understanding the impact of wind on the SPM concentration is beyond the focus of this study and should be investigated additionally.

We included the updated Pearson correlated matrix in the Appendix, and added this resumé to the methods and discussion sections:

Section 2:

“To have idea of the large-scale estimates of the wind impact on the annual cumulated SPM, we included the number of days of storms parameter.

Section 3:

“Another question that was not addressed in our study is the impact of the wind-induced mixing on the offshore SPM concentration. The simple hypothesis proposes that the higher is the wind speed, the more mixing occurs in a shallow area, which reduces the surface SPM concentrations. At the same time, an additional hypothesis may suggest that more mixing means more re-suspension of particulate matter from the bottom sediments (increasing the SPM concentration). To verify these controversial hypotheses, we have to compare quasi simultaneous wind and SPM observations. In case of this study, this problem faces a fundamental limitation due to the nature of a satellite-retrieved SPM dataset: the highest wind speeds are observed during the cyclone passage, and SPM concentrations cannot be retrieved from satellite data under the clouds (as clouds mask the water-leaving signal).

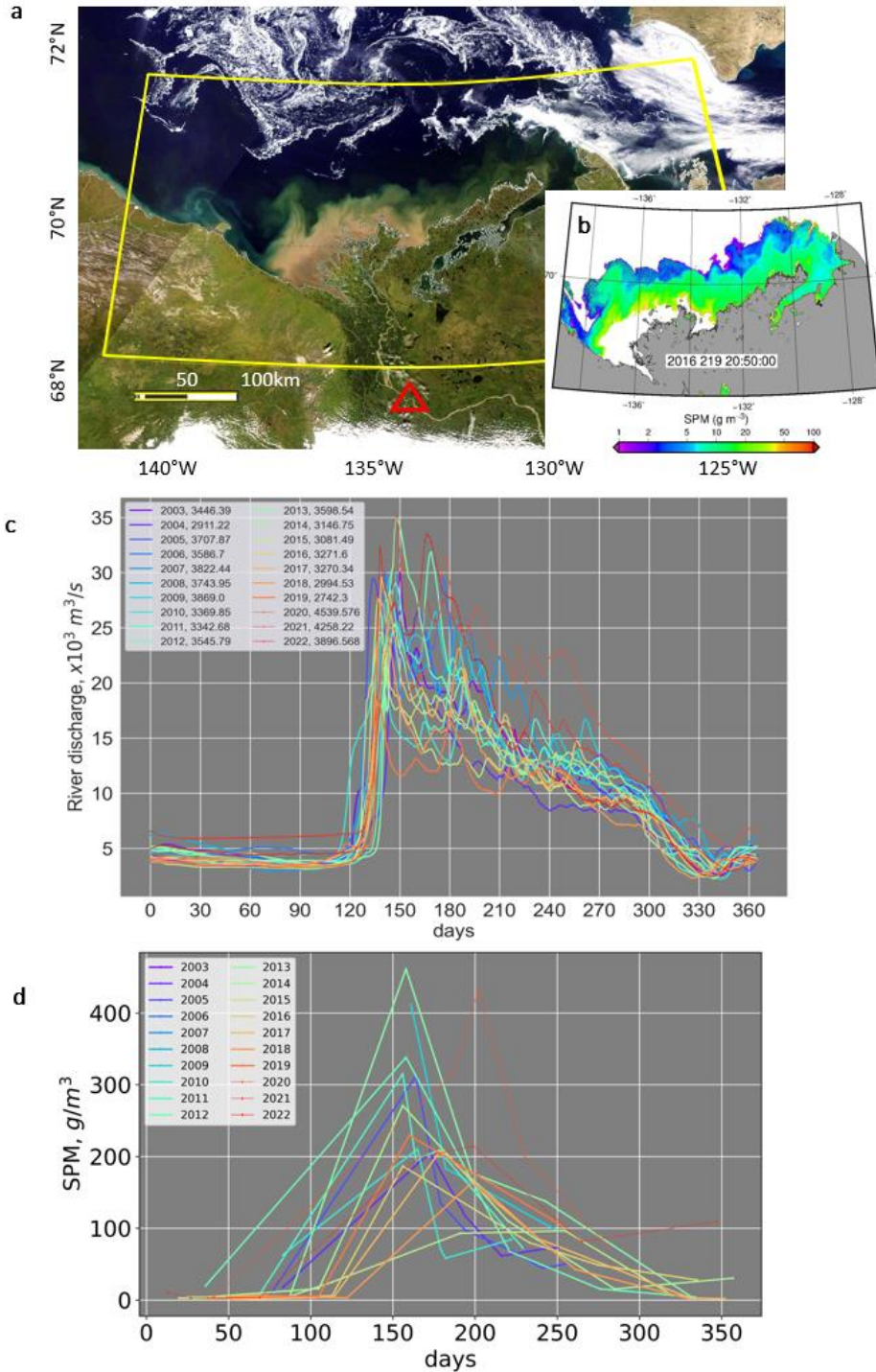
We found a weak negative correlation (correlation coefficient is -0.19) between the number of days of storm and annual cumulated SPM, which confirms the first simple hypothesis (more mixing, less SPM), but this question should be addressed additionally with other tools, like modeling.”



In conclusion, the issue is quite complex, and the statistical significance of the (linear) regressions is not very strong. As for the detailed comments:

1. Fig. 1: The map and satellite image should have a scale.

Thank you, we added a scale in Fig.1a:



2. The link to ERA5-LAND is incorrect (it should end with "...documentation").

Thank you for your suggestion, the new link was changed to <https://confluence.ecmwf.int/display/CKB/ERA5%3A+data+documentation> and <https://confluence.ecmwf.int/display/CKB/ERA5-Land%3A+data+document>

We were following the instruction found at <https://confluence.ecmwf.int/display/CKB/How+to+acknowledge+and+cite+a+Climate+Data+Store+%28CDS%29+catalogue+entry+and+the+data+published+as+part+of+it>

3. Fig. 2: Subfigures c and e, as well as d and f, have the same subtitle, but they describe different things. This is explained in the figure caption, but it's a bit confusing - please revise.

The titles were changes, thank you for your suggestions.

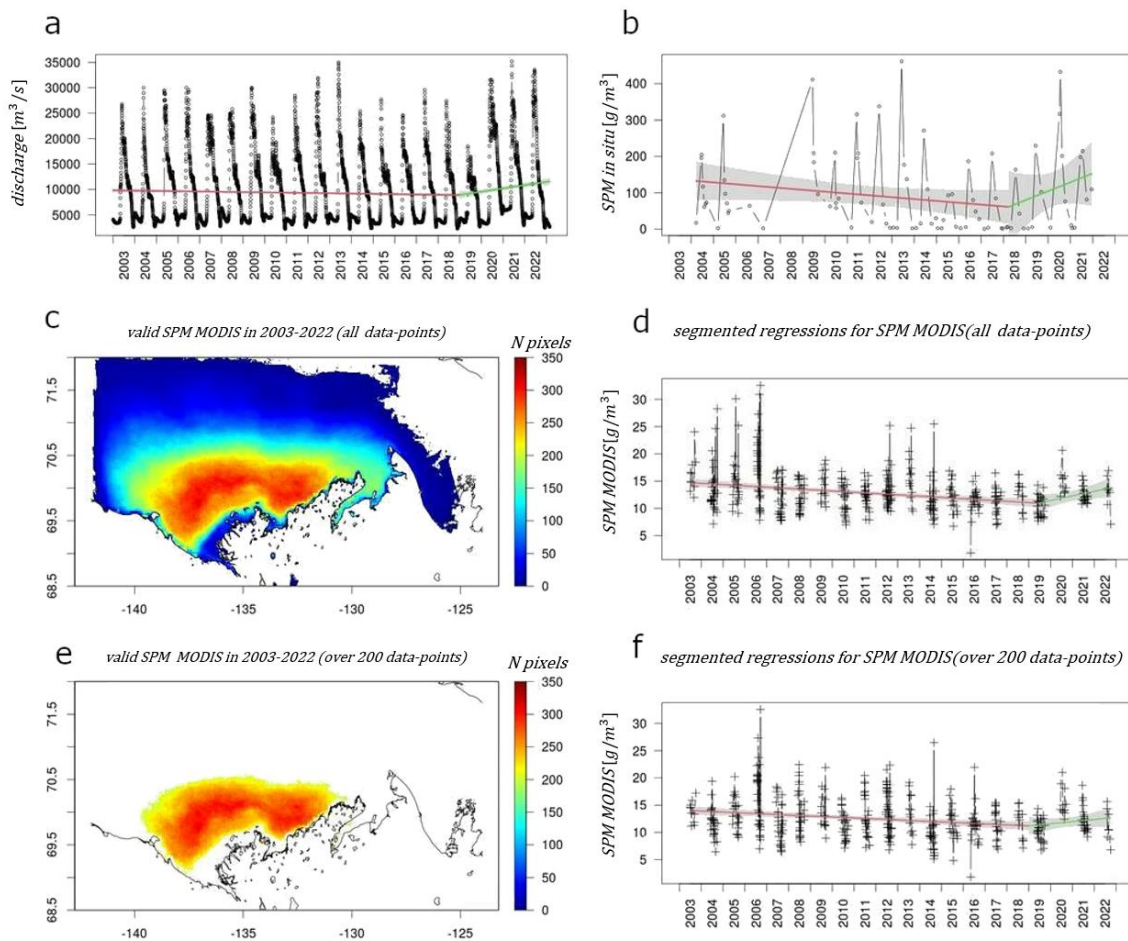


Fig.2

## Highlights

### **Variations of suspended particulate matter concentrations of the Mackenzie River plume (Beaufort Sea, Arctic Ocean) over the last two decades**

Anastasia Tarasenko, David Doxaran, Bernard Gentili

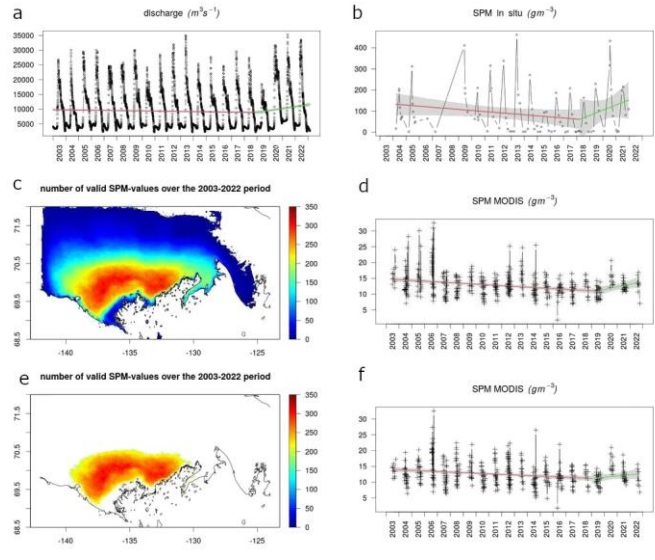
- Interannual variations of suspended particulate matter (SPM) in coastal waters influenced by the Mackenzie River were investigated over the last 20 years (2003-2022) using MODIS/Aqua satellite data
- The offshore SPM variations are related to the Mackenzie River hydrological regime, air temperature, amount of snow, and permafrost state over its draining basin
- Over the last twenty years, a statistically significant negative trend was highlighted over the period 2003-2018 for both SPM and river discharge, with a positive trend starting from 2019 up to present



# Graphical Abstract

## Variations of suspended particulate matter concentrations of the Mackenzie River plume (Beaufort Sea, Arctic Ocean) over the last two decades

Anastasia Tarasenko, David Doxaran, Bernard Gentili



1  
2  
3  
4  
5  
6  
7  
8  
9  
10  
11  
12  
13  
14  
15  
16  
17  
18  
19  
20  
21  
22  
23  
24  
25  
26  
27  
28  
29  
30  
31  
32  
33  
34  
35  
36  
37  
38  
39  
40  
41  
42  
43  
44  
45  
46  
47  
48  
49  
50  
51  
52  
53  
54  
55  
56  
57  
58  
59  
60  
61  
62  
63  
64  
65

1  
2  
3  
4  
5  
6  
7  
8  
9  
10  
11  
12  
13  
14  
15  
16  
17  
18  
19  
20  
21  
22  
23  
24  
25  
26  
27  
28  
29  
30  
31  
32  
33  
34  
35  
36  
37  
38  
39  
40  
41  
42  
43  
44  
45  
46  
47  
48  
49  
50  
51  
52  
53  
54  
55  
56  
57  
58  
59  
60  
61  
62  
63  
64  
65

## Highlights

### **Variations of suspended particulate matter concentrations of the Mackenzie River plume (Beaufort Sea, Arctic Ocean) over the last two decades**

Anastasia Tarasenko, David Doxaran, Bernard Gentili

- Interannual variations of suspended particulate matter (SPM) in coastal waters influenced by the Mackenzie River were investigated over the last 20 years (2003-2022) using MODIS/Aqua satellite data
- The offshore SPM variations are related to the Mackenzie River hydrological regime, air temperature, amount of snow, and permafrost state over its draining basin
- Over the last twenty years, a statistically significant negative trend was highlighted over the period 2003-2018 for both SPM and river discharge, with a positive trend starting from 2019 up to present

# Variations of suspended particulate matter concentrations of the Mackenzie River plume (Beaufort Sea, Arctic Ocean) over the last two decades

Anastasia Tarasenko<sup>a</sup>, David Doxaran<sup>a</sup>, Bernard Gentili<sup>a</sup>

<sup>a</sup>Laboratoire d'Océanographie de Villefranche UMR 7093 CNRS Sorbonne Université 06230 Villefranche-sur-Mer France

---

## Abstract

This work addresses the last 20 years' evolution of the suspended particulate matter (SPM) concentrations in the Beaufort Sea (Canadian Arctic Ocean) directly influenced by the Mackenzie River discharge. The SPM variations in the coastal zone are highlighted and related to the freshwater and solid discharges of the river measured in situ at the Arctic Red River station (150 km upstream of the river delta). The correlation between the variations of the river discharge and SPM concentration within the surface layer of the coastal waters is obvious. Rather unexpectedly, both have been slightly but significantly decreasing from 2003 to 2018-2019 and started to increase very recently (2019-2022). This change of regime could be explained by changing winter precipitation and groundwater distribution, progressively accumulating sediments within the thawing permafrost layer and its recent release into the groundwater together with thermokarst lakes' rapid drainage.

*Keywords:* suspended particulate matter, ocean optics, Arctic Ocean, MODIS

---

## 1. Introduction

Climate change occurs faster in polar regions than at lower latitudes Arias et al. (2021). Global warming is usually associated in high latitudes with rising air temperature, precipitations, and permafrost thaw Miner et al. (2022); Pörtner et al. (2022). Consequently, the freshwater discharged by rivers into the Arctic Ocean is expected to increase, so as the discharge of terrestrial substances with enhanced erosion along drainage basins Doxaran et al. (2015); Matsuoka et al. (2022); Juhls et al. (2022). This would result in increasing water turbidity in coastal areas directly affected by river inputs but also boosted primary production due to higher nutrient loads and reduced sea ice cover (i.e., increasing solar light within the water column).

1  
2  
3  
4 The Mackenzie River is the fourth largest Arctic river in terms of river discharge (7% of  
5 freshwater inflow to the Arctic Ocean) and is the primary source of sediment discharge  
6 Carson et al. (1998); Wagner et al. (2011); Yang et al. (2015), so the changes in the  
7 Mackenzie River regime will have a significant impact on the whole Arctic region Juhls et al.  
8 (2022). The Mackenzie has a prominent seasonal cycle with winter lows and a summer  
9 maximum of river discharge, which is related to the water cycle over its large basin with its  
10 75% permafrost area and the importance of snowmelt in spring Yang et al. (2015); Grotheer  
11 et al. (2020). The delta of the Mackenzie River is a complex area where the freshwater  
12 massively inflows into the southern Beaufort Sea, highly impacted by a long presence of sea  
13 ice. The southern Beaufort Sea is frozen most part of the year; the polynia between the fast  
14 ice of the delta starts opening in May, then the water surface stays mostly icefree from July  
15 to October. Over the last two decades, the sea ice conditions have become softer, and the sea  
16 ice concentration (SIC) has diminished by -4-8% per decade from 2003 to 2019 Hilborn  
17 and Devred (2022).

23 The open discussion of the Mackenzie River regime and its adaptation to climate change  
24 depends on the studied period Woo and Thorne (2003); Doxaran et al. (2015); Yang et al.  
25 (2015); Matsuoka et al. (2022); Zolkos et al. (2022). Doxaran et al. 2015 claimed a 22%  
26 increase of the river discharge from 2003 to 2013. Yang et al. 2015 showed that over the  
27 1973-2011 period, the positive linear trend for the Mackenzie discharge was very weak ( $y =$   
28  $17.21x + 8947.4$ ), and Woo and Thorne 2003 found no significant trend for the annual  
29 discharge over the period 1968-1999, nor did Matsuoka et al. 2022 for the 1992-2018  
30 period. Meanwhile, several studies agreed that the yearly amount of river discharge has  
31 changed its seasonal distribution: cold season discharge becomes slightly higher, but spring  
32 flows are lower (as higher air temperatures shift the snowmelt earlier) Woo and Thorne  
33 (2003); Yang et al. (2015). The question of the river water discharge, thus, should be  
34 regularly reevaluated.

39 In such a remote and changing environment, satellite observations have been proven to  
40 be an efficient tool to monitor the evolution of Arctic coastal zones, and compensate the  
41 lack of field measurements Doxaran et al. (2012); Hill et al. (2013); Juhls et al. (2022). SPM  
42 field measurements, although extremely valuable, are usually too sparse for the long-term  
43 variability analysis, as most of them are associated with specific summer expeditions (e.g.  
44 the recent MALINA Massicotte et al. (2021) and Nunataryuk Lizotte et al. (2023) field  
45 campaigns). Overall, during the ice-free season, satellite-derived suspended particulate  
46 matter (SPM) concentrations typically vary from  $30 \text{ g/m}^3$  in the delta region to  $0.5 \text{ g/m}^3$   
47 offshore over the Canada Basin Hilborn and Devred (2022).

51 Several studies analyzed satellite-derived SPM concentration variability in the southern  
52 Beaufort Sea for long time periods (over 10 years), and their results are rather  
53 controversial. From 2003 to 2013, Doxaran et al. 2015 found a linear trend with a significant  
54 increase in monthly- averaged SPM concentrations at the mouth of Mackenzie River (+46%  
55 in 10 years over the river mouth area and +71% in the river delta south to  $70^\circ\text{N}$ ). Hilborn  
56

60  
61  
62  
63  
64  
65



1  
2  
3  
4 and Devred 2022 applied *self-organizing maps* method to identify six different regions in  
5 the eastern Beaufort Sea using 17 years of MODIS (Moderate Resolution Imaging  
6 Spectroradiometer) data and found only one statistically significant trend (negative) for the  
7 annual SPM concentration in the deepwater Canada basin area, far offshore the Mackenzie  
8 delta. At the same time, Matsuoka et al. 2022 showed a statistically significant increase of  
9 dissolved and particulate organic matter concentrations (but not fluxes) in late summer:  
10 0.019  $g/m^3$  per year and 0.069  $g/m^3$  per year, accordingly).

11 The present study is a continuation of Doxaran et al.2015, where we analyze the  
12 evolution of the SPM concentration in the Beaufort Sea directly influenced by the discharge  
13 of the Mackenzie River over the last two decades (2003-2022), using the methodology  
14 developed by Doxaran et al. (2012, 2015), this time excluding the complex river delta zone.

## 20 21 **2. Materials and Methods**

22 Fig.1a shows the limits of the study area (yellow rectangular) on a quasitrue color daily  
23 MODIS composite for August 8, 2016. In this image, the SPM-rich Mackenzie River plume  
24 propagates along the coast and northward, partly into the MIZ (marginal ice zone). The  
25 variations of SPM concentrations (Fig.1b) from the delta to offshore waters are obvious,  
26 which highlights complex processes along this land-sea interface. The field and satellite  
27 datasets used in this study, so as the methods used to retrieve and analyze time series of  
28 river discharge and SPM concentrations, are detailed hereafter.

### 29 30 31 32 33 *2.1. Field data sets*

34 In situ measurements of the river water discharge (2003-2022) were provided by the  
35 Water Survey of Canada via the ArcticGRO project McClelland et al. (2023) at the Arctic Red  
36 River gauge station (station ID: 10LC014, 67.45°N 133.74°W, red triangle in Fig.1a). River  
37 discharge measurements,  $Q$ , are available daily (Fig.1c). The measurements of suspended  
38 matter are distributed by the ArcticGRO as *total suspended solids (TSS)* concentrations,  
39 which is the same as SPM, so hereafter we will refer to in situ TSS as the  
40  $SPM_{insitu}$ . The  $SPM_{insitu}$  data were collected at most once per month, but not during all months  
41 (on average, 4 to 6 measurements per year, Fig.1d). Over the studied period, some years are  
42 poorly represented (one measurement per year in 2003, 2006, and 2007; no SPM  
43 measurement in 2008). The lack of SPM in situ data implies the necessity to use satellite  
44 data.

45 The ArcticGRO in situ datasets pass the quality control procedure and indicate less  
46 reliable measurements as "provisional data". Over the 2003-2022 period, it corresponds to  
47 river discharge data in 2020-2022 and  $SPM_{insitu}$  data in 2019-2022 (shown with thinner  
48 lines in Fig.1c, d).

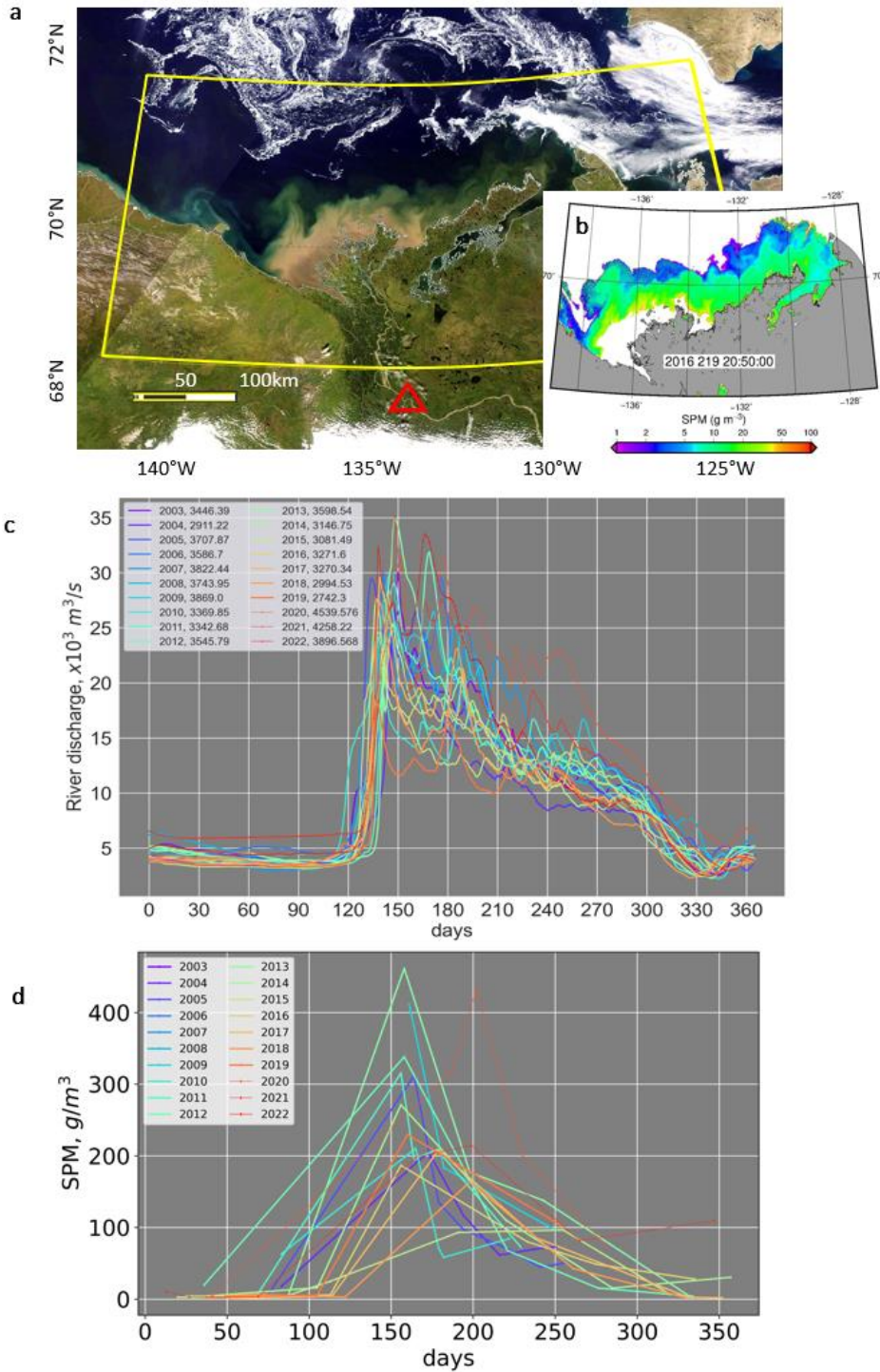


Figure 1: (a) MODIS image (August 6, 2016) locating the Arctic Red River gauge station (Tsiigehtchic) where in situ measurements are carried out (red triangle) and the coastal waters studied using satellite data (yellow rectangle); (b) SPM concentrations: Interannual variations of water discharge (the year of measurement and the annual cumulative sum of discharge is indicated in legend), (c) and SPM concentrations (d) at the Arctic Red River station. The inserted SPM color map shows the result of MODIS satellite data processing

1  
2  
3  
4  
5  
6  
7 *2.2. Ocean color satellite data*

8 As in Doxaran et al. 2015, a single satellite sensor (MODIS/Aqua) was considered for  
9 this study in order to avoid any bias between different sensor products when detecting  
10 temporal trends. Since 2003, MODIS provides high-quality ocean color observations at a  
11 good temporal resolution: several images per day of the study area during the Arctic  
12 summer months Doxaran et al. (2012, 2015); Hilborn and Devred (2022); Matsuoka et al.  
13 (2022). The region of interest was defined as 68.5°N-72°N, 142°W - 124°W (yellow  
14 rectangle in Fig.1a). The initial dataset contained 10608 swaths collected between May 1  
15 and October 31 each year over the 2003-2022 period.  
16

17  
18 *Processing of satellite data.* MODIS L1A satellite data were processed using the SeaWiFS  
19 Data Analysis System (SeaDAS 8.1.0) software (<http://seadas.gsfc.nasa.gov/>) and its l2gen  
20 function. The atmospheric correction was performed using the NIR-SWIR algorithm of  
21 Wang and Shi 2007); this method was proved to be the most appropriate for the highly  
22 turbid waters at the mouth of the Mackenzie River to the less turbid waters offshore  
23 Doxaran et al. (2012).  
24

25  
26 SeaDAS l2gen flags were used to mask clouds and glint. In the work of Doxaran et al.  
27 2015, two techniques were used to mask clouds: the default one in the coastal waters and  
28 an increased cloud albedo threshold value (0.4 instead of 0.027) over the specific area of  
29 the river delta zone to avoid masking the highly turbid water pixels. This procedure was  
30 time-consuming and required an additional inspection of every image in the river delta  
31 zone. Here, the cloud-masking method preconized by Ody et al. 2022 for river mouths was  
32 used to process each satellite image only once: the 2130 nm shortwave-infrared waveband  
33 was used with a cloud threshold of 0.018. The sea ice mask was computed from daily sea  
34 ice concentration (SIC) data at 3.125°spatial resolution distributed by the University of  
35 Bremen Spreen et al. (2008). This dataset contains AMRS-E and AMSR2 (Advanced  
36 Microwave Scanning Radiometer -for Eos and -2) images. Due to several gaps in data  
37 acquisition over the 2003-2022 time period, the dataset was completed with the sea ice  
38 concentration from the SSMIS (Special Sensor Microwave Imager/Sounder) instrument.  
39 The ice mask was created using the SIC above 0%.  
40

41 All satellite data (Rayleigh-corrected reflectances and masks) were reprojected on a  
42 regular 250 m grid. The following criteria were then applied to exclude potentially  
43 contaminated images:  
44

- 45 • the number of valid pixels should exceed 15% of the marine area of the study area in  
46 the downloaded MODIS image;
  - 47 • the distance between the central point of the study area and that of the MODIS image  
48 should be less than 1000 km to avoid aberrations on the border of the image;
- 49  
50  
51  
52  
53  
54  
55  
56  
57  
58

- only areas with a zenith solar angle lower than 74° were conserved.

This automatic filtering reduced the MODIS collection to 700 images. Finally, all images were inspected visually to filter out the remaining contaminated images because of not detected MIZ, clouds or cloud shadows, etc.; 651 MODIS images remained after this last quality check step.

The SPM concentrations were computed from the ratio (in %) between the remote sensing reflectance signals,  $R_{rs}$  (in  $sr^{-1}$ ) in the near-infrared and green wavebands using the set of relationships established based on field measurements Doxaran et al. (2012, 2015):

$$SPM_{sat} = 0.8386 \times R_{RS}(748 : 555) \quad (1)$$

if  $R_{RS}(748 : 555) < 87\%$

$$SPM_{sat} = 70 + 0.1416 \times R_{RS}(748 : 555) + 2.9541 \times e^{0.2092 \times (R_{RS}(748:555) - 87)} \quad (2) \text{ if } 87\% \leq R_{RS}(748 : 555) \leq 94\%$$

$$SPM_{sat} = 3.922 \times R_{RS}(748 : 555) - 285.4 \quad (3)$$

if  $94\% < R_{RS}(748 : 555)$ , where  $SPM_{sat}$  is the SPM concentration in  $g/m^3$  and  $R_{RS}(748 : 555)$  is the ratio of remote-sensing reflectances at 748 and 555 nm.

Negative  $R_{RS}(555)$  and  $R_{RS}(748)$  values were discarded before computing SPM, as well as computed SPM concentrations higher than  $1000 g/m^3$ , to remove atmospheric correction failures and residual contaminations (typically encountered along borders of clouds or sea ice).

The processed SPM images were averaged as daily, monthly, and yearly composites as simple mean averages for every pixel. Only daily composites and their mean values were used further, as monthly composites were sometimes computed using only 1 to 3 cloud-free images, which is not representative of mean monthly concentrations.

### 2.3. Reanalysis data

A dataset from ERA5 Land reanalysis was extracted to better understand how environmental factors did impact the Mackenzie River discharge and SPM concentrations in the adjacent coastal waters. This dataset was selected as the most suitable tool for the studies of river discharge variability Winkelbauer et al. (2022). ERA5 Land has a monthly temporal resolution and 9-km spatial resolution and is provided by Copernicus data center Muñoz-Sabater et al. (2021). The area of extraction approximately corresponds to the Mackenzie drainage basin (52-70°N, 100-140°W). The following parameters were used: river runoff (ro), surface river runoff (sro), evaporation (e), total precipitation (tp), snow depth (sd), and air temperature at 2m (t2m), (see detailed description at <https://confluence.ecmwf.int/display/CKB/ERA5-Land%3A+data+document> The

1  
2  
3  
4 Pearson correlation matrix for the mean annual values of all described parameters  
5 (Fig.A.3).  
6

7 To include a possible effect of storms on the SPM concentrations, we added to the  
8 analysis the wind data from ERA5 (marine area similar to that chosen for the MODIS study  
9 box). The Pearson correlation matrix (where the yearly parameters are compared) contains  
10 an additional parameter "the number of days of storms per year" (*ndays\_storm* in Fig. A.3).  
11 The day was considered stormy if over the study area there was a wind vector with a wind  
12 speed over 15 m/s.  
13  
14

#### 15 2.4. Temporal variability

16 As previous works have shown, the linear regression model provides relatively little  
17 information on interannual variability of river water discharge and related parameters,  
18 such as SPM, because, over the long term, the discharge appears as stable Yang et al. (2015);  
19 Matsuoka et al. (2022). Over the last 20 years, the linear trend for the in situ Mackenzie  
20 discharge time series calculated with the Ordinary Least Squares (OLS) model is  $y =$   
21  $17.1x + 9554$  with a standard error (SE) of  $63.6 \text{ m}^3/\text{s}$ , and confidence intervals (CI) [0.025  
22 0.975] equal to  $-107.5$  and  $141.7 \text{ m}^3/\text{s}$  for the coefficient term. Although these results are  
23 very close to that of Yang et al. 2015, the statistical metrics confirm that the OLS model is  
24 not suitable for the analysis in this case.  
25  
26  
27

28 For this reason, we used an estimating regression model with unknown break-points,  
29 which allows describing several temporal trends Muggeo (2003). To apply this model to  
30 our datasets, we used the *segmented* function in the R package *segmented*.  
31

32 To compute the trends, the in situ data time series of daily river discharge ( $Q_{insitu}$ ) and  
33 SPM concentration ( $SPM_{insitu}$ ) described above were used (Fig.2a, b). For the satellite data,  
34 the spatial sparsity of observations was taken into account. Thus, to obtain  $SPM_{sat}$  time  
35 series, we calculated: • one daily spatial mean SPM value for all available SPM pixels over  
36 the study area, which resulted in  $SPM_{sat}$  time series (Fig.2 c-d); • one daily spatial mean SPM  
37 value for the area with the highest data density (where valid satellite pixels appear more  
38 than 200 times over the 2003-2022 period), which resulted in  $SPM_{sat200}$  (Fig.2 e-f)  
39  
40  
41  
42  
43  
44

45 Then the segmented regression analysis technique was applied to all time series:  $Q_{insitu}$ ,  
46  $SPM_{insitu}$ ,  $SPM_{sat}$ , and  $SPM_{sat200}$ . After several tests, the most statistically significant results  
47 were obtained with one breaking point and two segment slopes. The following statistical  
48 parameters were computed for each segment: estimated coefficient of linear regression  
49 (Est.), standard error, lower and upper 95% confidence intervals (CI(95%).l, CI(95%).u,  
50 respectively) (Tab.1).  
51  
52  
53  
54  
55  
56  
57  
58

### 3. Results and Discussion

The seasonal cycles of both the river discharge,  $Q$ , and  $SPM_{insitu}$  are very pronounced, with high summer and low winter values (Fig.1c,d). These parameters also have a strong interannual variability. During the 2003-2022 period, the river discharge varied from  $2.2 \times 10^3 \text{ m}^3/\text{s}$  (winter) to  $35.2 \times 10^3 \text{ m}^3/\text{s}$  (summer), with a mean value of  $9.5 \pm 6.8 \times 10^3 \text{ m}^3/\text{s}$ . Typically, the discharge increases very rapidly in 2 weeks from 5 to  $25 \times 10^3 \text{ m}^3/\text{s}$  in late May, when the main summer peak occurs, then slowly decreases to its winter values by November.

The years 2013 and 2021 were exceptional with extreme *yearly maxima* of river discharge over  $35 \times 10^3 \text{ m}^3/\text{s}$  on May 28 (both), while the lowest yearly maximum river discharge,  $18 \times 10^3 \text{ m}^3/\text{s}$ , was registered on May 18, 2019. Previously, Yang et al. 2015 also observed similar prominent interannual variations in the river discharge during the summer (e.g., in 1992 and 1995 for the 1972-2011 period). They concluded that a negative anomaly in precipitation-evaporation balance over the river basin in summer (hot and dry weather) usually results in a lower discharge the next year with an earlier maximum, while the opposite (cold and wet) weather is responsible for a higher discharge. This statement does not explain the extreme peak of discharge recorded in 2013: in 2012 the summer was “hot and dry”, so 2013 should have been a year of extremely low summer river discharge. Overall, calculated correlations between in situ river discharge and ERA5 Land total precipitation, as well as air temperature were weak (0.36 and -0.23, respectively). However, the river discharge is well correlated with snow depth cover (correlation coefficient between  $Q_{insitu}$  and  $sd$  is 0.67): the 2011-12 and 2012-13 winters were snowy (+10% and +3%  $sd$  anomaly compared to 20years median values), as well as the 2020 winter (+7%  $sd$  anomaly), but 2018-19 snow cover was weak (-7%  $sd$  anomaly). Interestingly, in 2013 the yearly means of river discharge and air temperature were close to their 20years median values, indicating the overall stability of the system during this period.

The river discharge regime in 2006-2008 and 2012 was special with two summer  $Q$  maxima, the first one in late May and the second between the end of June and mid-July. The reason for this change in river regime might be related to the precipitation seasonal pattern and the river ice opening (several ice jams crushes, creating the second peak). To investigate these particularities, a higher temporal resolution reanalysis data should be used. We also observe local maxima (values higher than the previous year) in  $SPM_{sat}$  in 2006, 2008, and 2012.

As explained in section 2.4, the OSL model does not highlight a statistically significant trend in the river discharge time series, but the *segmented* model does. Fig.2 and Table 1 present the results of calculated segmented regressions, where the river discharge and SPM concentrations demonstrate very similar trends: a negative trend from 2003 to 2018, then a recent positive trend from 2019 (2018 for  $SPM_{insitu}$ ) to 2022 (Fig.2). Based on the

1  
2  
3  
4 confidence intervals, we conclude that negative trends for  $slope1_Q$ ,  $slope1_{SPM_{sat}}$ , and  
5  $slope1_{SPM_{sat200}}$  are statistically significant (CIs [0.025 0.975] are all negative).  
6

7 This negative trend of  $slope1_Q = -57.21x + const$  in river discharge for the 2003-2018  
8 period is opposite to that of Doxaran et al. 2015 for the 2003-2013 period, but the latter  
9 study slightly overestimated the river discharge in 2013 (as the data was not yet fully  
10 quality-checked) resulting in an erroneous positive (+22%) trend. As already mentioned,  
11 other studies, e.g. Yang et al. (2015); Matsuoka et al. (2022) which used an OSL model did  
12 not find any significant trend in the Mackenzie River discharge. The positive trend from  
13 2019 to the present,  $slope2_Q = 640.05x + const$ , although not statistically significant, can  
14 indicate a progressive increase in the minimum flow impacted by a "mobilization of ground  
15 waters" as discussed by Yang et al. 2015.  
16  
17  
18

19 In situ data show that the SPM seasonal cycle generally follows the river discharge cycle,  
20 with the summer maxima in late May - beginning of June. The  $SPM_{sat}$  values vary from 0.8  
21 to  $461 \text{ g/m}^3$  with a median value of  $67.7 \pm 11 \text{ g/m}^3$ . The breakpoint of  $SPM_{isitu}$  trends is  
22 slightly shifted to 2018, and CIs contain zero, thus indicating that the *segmented* model is  
23 less reliable for this dataset. At the same time, the  $SPM_{isitu}$  time series has the fewest amount  
24 of data, which is not homogeneous in time and is mainly available in summer. It makes it  
25 more difficult to interpret with any statistical model.  $SPM_{sat}$  and  $SPM_{sat200}$  trend analyses  
26 show similar results: their negative  $slope1$  values and corresponding SE are close to each  
27 other, which gives confidence in the observed SPM negative trend. The positive trends  
28  $slope2_{sat}$  and  $slope2_{sat200}$  are not statistically significant, and their SEs are of the order of the  
29 estimated coefficient of linear regression (Tab.1). Nevertheless, this result is interesting for  
30 further discussion.  
31  
32  
33  
34

35 Over the 2003-2019 period, Hilborn and Devred 2022 obtained results in good  
36 agreement with a negative trend (although not significant) for SPM concentrations over the  
37 southern Beaufort Sea (from -0.16 to  $-0.46 \text{ g/m}^3$  per decade) except for the Mackenzie River  
38 delta, where they found an increase of SPM of  $0.36 \text{ g/m}^3$  per decade. The difference in  
39 negative coefficients' values obtained in the present study and that of Hilborn and Devred  
40 (2022) comes from (1) the difference of SPM-retrieval methods and different MODIS bands  
41 used; and (2) the regions: our study region of  $SPM_{sat200}$  corresponds to 3 regions over the  
42 shelf identified by Hilborn and Devred (2022).  
43  
44  
45

46 In the Mackenzie delta zone, Doxaran et al. 2015 also found a significant increase of SPM  
47 (+71% from 2003 to 2013) over the "Mackenzie River delta" region of Hilborn and Devred  
48 (2022). The delta zone seems to play an important role of "SPM filter" between the river  
49 and the coastal waters. Based on satellite observations, SPM apparently settles massively  
50 in this shallow area, resulting in the formation of temporary maximum turbidity zones  
51 where resuspension of bottom sediments may occur depending on the river discharge, tidal  
52 currents, and wind stress (Wegner et al., 2005; Grotheer et al., 2020). Observations at high  
53 spatial and temporal resolutions are required to further investigate SPM dynamics in this  
54 delta zone.  
55  
56  
57  
58

1  
2  
3  
4 However, how to explain the negative trends in both river discharge and SPM  
5 concentrations in the riverbed and offshore delta zone over the 2003-2018 period? Based  
6 on the correlation matrix (Fig. A.3), we recognize that the river runoff and, thus, river  
7 discharge variability depend mostly on the amount of total precipitation ( $r = 0.7$ ) and the  
8 snow depth ( $r = 0.63$ , which is another estimate of solid precipitation in winter)  
9 parameters. This trivial conclusion leads us to a simple suggestion that the Mackenzie River  
10 discharge slightly declined while the precipitation pattern has changed over this period.

11  
12 As for the SPM, the recent study of Zolkos et al. 2022 reveals a similar decrease in SPM  
13 loads in most of the Siberian rivers between 1970 and 2010 and explains it by natural and  
14 anthropogenic factors. The "natural factors" of sediments erosion over the river basin are  
15 the physical and chemical denudation. For the Mackenzie River, the physical denudation  
16 rates exceed the chemical denudation about several orders of time: mechanical denudation  
17 rate at the Arctic Great River was reported as  $844 \text{ t} \cdot \text{km}^{-2} \cdot \text{y}^{-1}$  in 1997, while the  
18 chemical weathering occurs at a rate of  $25 \text{ mm} \cdot \text{ky}^{-1}$  with a transport time of  $10\text{-}400 \text{ ky}^{-1}$   
19 (Vigier et al. (2001); DePaolo et al. (2006)). On the order of two decades, it is, thus, physical  
20 or mechanical factors related to the river discharge and the atmospheric conditions in the  
21 delta-adjacent areas that control SPM concentrations. A simultaneous decline of  $Q_{\text{insitu}}$   
22 and  $SPM_{\text{insitu}}$  in 2003–2018 means that the lower the river discharge, the less suspended  
23 particulate matter it transports.

24  
25 Another source of variability for the "marine" SPM might be the wind mixing. The simple  
26 hypothesis proposes that the higher the wind speed, the more mixing occurs in a shallow  
27 area, which reduces the surface SPM concentrations. At the same time, an additional  
28 hypothesis may suggest that more mixing means more re-suspension of particulate matter  
29 from the bottom sediments (increasing the SPM concentration). To verify these  
30 controversial hypotheses, we must compare quasi simultaneous wind and SPM  
31 observations. In the framework of this study there is yet one fundamental limitation for  
32 this analysis due to the nature of ocean color data retrieval from satellite: the highest wind  
33 speed (and thus mixing events) will mostly occur under the cloud cover with the passage  
34 of cyclones, and SPM concentrations cannot be retrieved from ocean color satellite under  
35 such conditions (presence of clouds). We found a weak negative correlation (correlation  
36 coefficient is  $r = -0.19$ ) between the number of days of storm and annual cumulated SPM,  
37 which confirms the first simple hypothesis (more mixing, less SPM), but this question  
38 should be addressed additionally with other tools, like modeling.

39  
40 There is yet a question about the recent positive trends in  $Q$  and  $SPM$  over the last 3-5  
41 years of observations. Although the trends are statistically not significant, can we suggest  
42 any important processes that might have impacted the river discharge and sedimentation  
43 transport recently?

44  
45 The presence of permafrost over the river basin was considered as "precluding" for the  
46 groundwater's contribution to general river discharge, as it prevented the water infiltration  
47 through the permafrost layer, but might have helped to create underground cavities filled  
48 with non-communication water reservoirs (Vigier et al. (2001)). With a progressive

50  
51  
52  
53  
54  
55  
56  
57  
58  
59  
60  
61  
62  
63  
64  
65



permafrost thawing, this neglected role might be re-evaluated. Matsuoka et al. 2022 observed an increase of thaw depth and precipitation, but a decrease in river discharge, which is probably explained by the contribution of ground waters, also suggested by Connolly et al. (2020). The permafrost thaw also likely affects the drainage of lakes located in the permafrost area Webb and Liljedahl (2023). A recent work of Nitze et al. 2020 described, e.g., a series of extremely quick thermokarst lakes drainage in 2018 in northwestern Alaska after the unprecedented warm (with air temperature close to 0°C) and wet winter of 2017-2018. This drainage "exceeded the average drainage rate by a factor of 10", and is supposed to continue and increase the liquid and solid discharges of Arctic rivers. This situation suggests that in the Canadian Arctic, where "large areas are susceptible to hillslope thermokarst activity" (Zolkos et al. (2022)), the permafrost thawing will progressively change chemical denudation and induce the downstream redistribution of sediments over the next millennial(s).

Table 1: Statistics for the segmented linear regression analysis of in situ river discharge (Fig.2a) -  $slope_Q$ ; trends of  $SPM_{insitu}$ :  $slope_{insitu}$  (Fig.2b); trends of  $SPM_{sat}$  for all available points:  $slope_{sat}$  (Fig.2d); and trends for  $SPM_{sat}$  for the area with over 200 pixels available:  $slope_{sat200}$  (Fig.2f). Negative trend parameters are described with  $slope1$ , positive with  $slope2$

	Est.	Standard error	CI(95%).l	CI(95%).u
$slope1_Q$	-57.21	19.14	-94.73	-19.68
$slope2_Q$	640.05	142.91	359.88	920.19
$slope1_{insitu}$	-5.08	3.04	-11.13	0.96
$slope2_{insitu}$	24.46	21.86	-19.02	67.93
$slope1_{sat}$	-0.23	0.04	-0.32	-0.15
$slope2_{sat}$	0.84	0.43	-0.01	1.70
$slope1_{sat200}$	-0.18	0.04	-0.27	-0.09
$slope2_{sat200}$	0.39	0.40	-0.40	1.18

#### 4. Conclusion

Twenty years (2003-2022) of in situ measurements (river discharge and SPM concentration at the Arctic Red River station) and satellite-derived SPM concentrations were analyzed to describe the evolution of SPM inputs in the Beaufort Sea by the Mackenzie River and its impact on the adjacent coastal waters. Using the segmented regression model, we showed two opposite trends over the last 20 years for both the river freshwater discharge and SPM concentration. Over the studied period, we observe statistically significant negative trends from 2003 to 2018-2019, then a positive trend from 2019 to 2022 for both river discharge and SPM concentrations. Our results extend previous estimations of Doxaran et al. 2015 and tend to confirm other long-term observations

1  
2  
3  
4 showing a rather stable freshwater discharge of the Mackenzie River, increasing SPM  
5 concentrations in the delta zone and a significant decrease in SPM concentration in  
6 adjacent coastal waters Feng et al. (2021); Hilborn and Devred (2022); Matsuoka et al.  
7 (2022).  
8

9  
10 We suggest that the observed variability indicates a simultaneous decline of water  
11 discharge and, thus, suspended particulate matter transport due to changing precipitation  
12 pattern, especially the amount of snow over the river basin with a possible role of wind-  
13 induced mixing in the marine area. We also discuss long-term effects of climate change  
14 and permafrost thawing on the sediment transport rate in the Mackenzie River.  
15

16 These processes of SPM release into the Arctic Ocean should be studied next on a pan-  
17 Arctic scale: can we expect a similar behavior based on the regional variations of river  
18 discharges reported by ArcticGRO? A recent study of Zolkos et al. 2022 used only in situ  
19 data, and further analysis of SPM distribution into the Arctic Ocean with satellite data will  
20 be beneficial. Studying the seasonal variability for specific years (e.g., 2006-2008, 2012) is  
21 also required using higher resolution data, including satellite imagery, to better understand  
22 changing river regimes in Arctic regions.  
23  
24  
25  
26  
27  
28  
29  
30  
31  
32  
33  
34  
35  
36  
37  
38  
39  
40  
41  
42  
43  
44  
45  
46  
47  
48  
49  
50  
51  
52  
53  
54  
55  
56  
57  
58

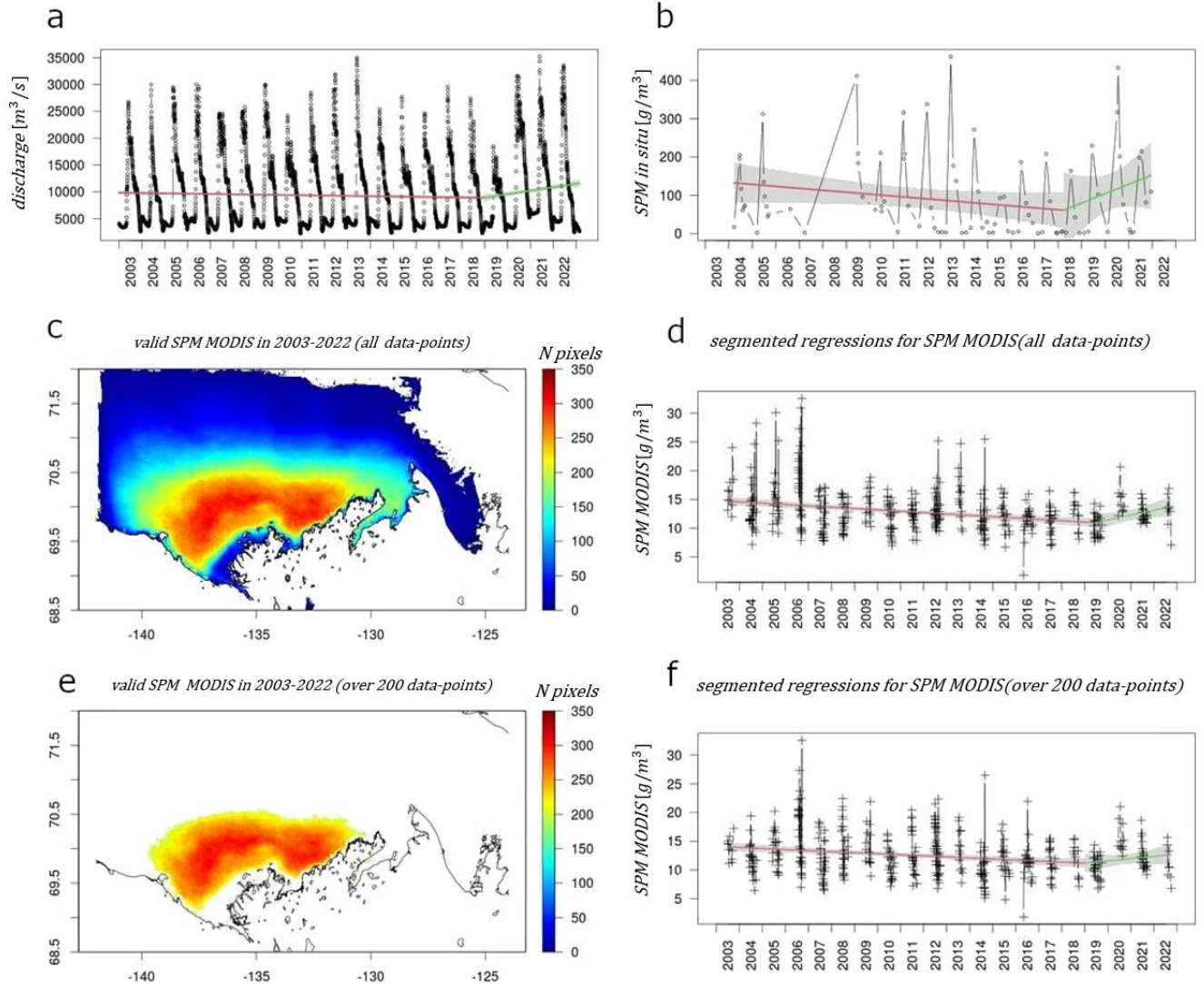


Figure 2: Interannual variations of in situ and satellite data (river discharge and SPM) with their segmented linear regression slopes (red and green colors show negative and positive regressions, respectively): (a) river discharge  $Q_{insitu}$ , (b)  $SPM_{insitu}$  time series; (c) maximum number of valid  $SPM_{sat}$  pixels in 2003-2022 (d) satellite  $SPM_{sat}$  time series; (e-f) similar to (c-d), but for the area with at least 200 valid pixels

## 5. Data availability

In situ measurements described in section 1 (river water discharge and TSS) are provided at <https://arcticgreatrivers.org/data/>. MODIS data is accessible from the NASA website <https://oceancolor.gsfc.nasa.gov>. Sea ice concentrations are available at <https://seaice.uni-bremen.de/data-archive/>. ERA5 LAND reanalysis data can be found at

1  
2  
3  
4 <https://doi.org/10.24381/cds.68d2bb30> with a detailed description at  
5 <https://confluence.ecmwf.int/display/CKB/ERA5%3A+data+documentation>, and ERA5  
6 wind data is available at <https://doi.org/10.24381/cds.adbb2d47> with a detailed  
7 description at  
8

## 9 **6. Acknowledgments**

10  
11 This study is part of the Nunataryuk project. The project has received funding under the  
12 European Union's Horizon 2020 Research and Innovation Program under grant agreement  
13 no. 773421. The study was co-funded by the ArcticFlux TOSCA project from the French  
14 space agency (CNES). The authors want also to acknowledge the NASA Goddard Space  
15 Flight Center, Ocean Ecology Laboratory, Ocean Biology Processing Group.  
16 Moderateresolution Imaging Spectroradiometer (MODIS) Aqua Data; NASA OB.DAAC,  
17 Greenbelt, MD, USA. doi: DOI. Accessed on 05/08/2023.  
18

19 No conflict of interest is stated.  
20  
21  
22

## 23 **Appendix A. ERA5-Land**

24  
25 The appendix contains Fig.A.3 illustrating correlation between ERA5 parameter, the  
26 Mackenzie discharge from the Arctic GRO dataset, and in situ and satellite SPM  
27 concentrations.  
28  
29  
30  
31  
32  
33  
34  
35  
36  
37  
38  
39  
40  
41  
42  
43  
44  
45  
46  
47  
48  
49  
50  
51  
52  
53  
54  
55  
56  
57  
58

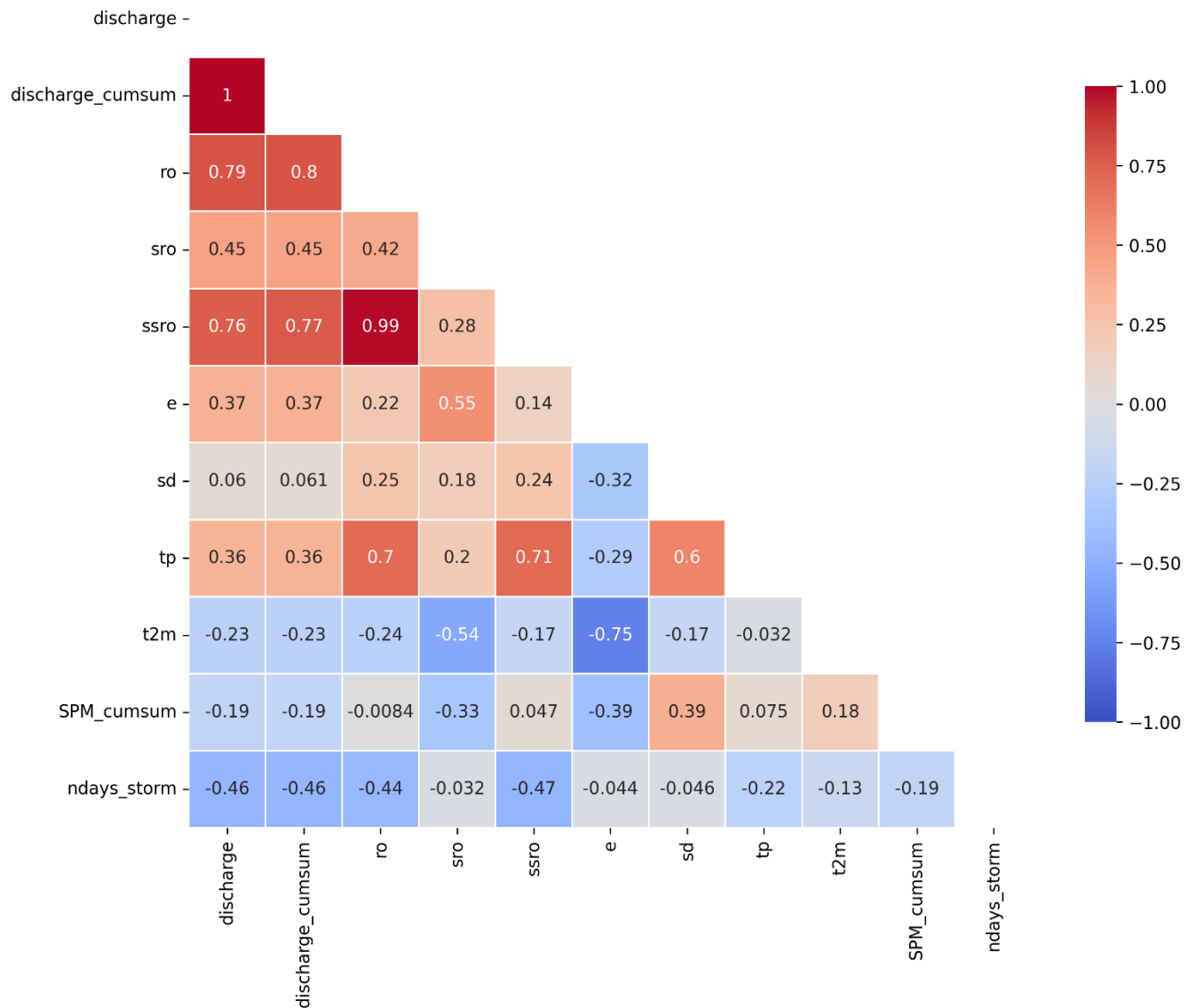


Figure A.3: Correlation matrix of all mean yearly reanalysis (ERA5 LAND) parameters over the Mackenzie basin and in situ (Arctic GRO) discharge for Mackenzie (Arctic Red station). ERA5 Land parameters are described in main text (ro - total runoff, sro surface runoff, ssro - subsurface runoff (ssro = ro-sro), e - evaporation, sd - snow depth, tp - total precipitation, t2m - air temperature at 2 m,  $SPM_{cumsum}$  - annual cumulated SPM concentrations, discharge - Arctic GRO in situ discharge).

## References

Arias, P., Bellouin, N., Coppola, E., Jones, R., Krinner, G., Marotzke, J., Naik, V., Palmer, M., Plattner, G.K., Rogelj, J., et al., 2021. Climate Change 2021: the physical science basis. Contribution of Working Group I to the Sixth Assessment Report of the

1  
2  
3  
4 Intergovernmental Panel on Climate Change; technical summary. Technical Report. IPCC.  
5 Geneva, Switzerland.  
6

7  
8 Carson, M., Jasper, J., Conly, F.M., 1998. Magnitude and sources of sediment input to the  
9 Mackenzie delta, northwest territories, 1974–94. *Arctic* , 116– 124.  
10

11 Connolly, C.T., Cardenas, M.B., Burkart, G.A., Spencer, R.G., McClelland, J.W., 2020.  
12 Groundwater as a major source of dissolved organic matter to arctic coastal waters.  
13 *Nature Communications* 11, 1479.  
14

15  
16 DePaolo, D.J., Maher, K., Christensen, J.N., McManus, J., 2006. Sediment transport time  
17 measured with u-series isotopes: results from odp north atlantic drift site 984. *Earth and*  
18 *Planetary Science Letters* 248, 394–410.  
19

20  
21 Doxaran, D., Devred, E., Babin, M., 2015. A 50% increase in the mass of terrestrial particles  
22 delivered by the Mackenzie river into the beaufort sea (Canadian arctic ocean) over the  
23 last 10 years. *Biogeosciences* 12, 3551– 3565.  
24

25  
26 Doxaran, D., Ehn, J., B'elanger, S., Matsuoka, A., Hooker, S., Babin, M., 2012. Optical  
27 characterisation of suspended particles in the mackenzie river plume (canadian arctic  
28 ocean) and implications for ocean colour remote sensing. *Biogeosciences* 9, 3213–3229.  
29

30  
31 Feng, D., Gleason, C.J., Lin, P., Yang, X., Pan, M., Ishitsuka, Y., 2021. Recent changes to arctic  
32 river discharge. *Nature communications* 12, 6917.  
33

34  
35 Grotheer, H., Meyer, V., Riedel, T., Pfalz, G., Mathieu, L., Hefter, J., Gentz, T., Lantuit, H.,  
36 Mollenhauer, G., Fritz, M., 2020. Burial and origin of permafrost-derived carbon in the  
37 nearshore zone of the southern canadian beaufort sea. *Geophysical Research Letters* 47,  
38 e2019GL085897.  
39

40  
41 Hersbach, H., Bell, B., Berrisford, P., Biavati, G., Horányi, A., Muñoz Sabater, J., Nicolas, J.,  
42 Peubey, C., Radu, R., Rozum, I., Schepers, D., Simmons, A., Soci, C., Dee, D., Thépaut, J-N.  
43 (2023): ERA5 hourly data on single levels from 1940 to present. Copernicus Climate  
44 Change Service (C3S) Climate Data Store (CDS), DOI: [10.24381/cds.adbb2d47](https://doi.org/10.24381/cds.adbb2d47) (Accessed  
45 on 07-SEP-2023)  
46

47  
48 Hilborn, A., Devred, E., 2022. Delineation of eastern beaufort sea subregions using self-  
49 organizing maps applied to 17 years of modis-aqua data. *Frontiers in Marine Science* ,  
50 1061.  
51

52  
53 Hill, V.J., Matrai, P.A., Olson, E., Suttles, S., Steele, M., Codispoti, L.A., Zimmerman, R.C., 2013.  
54 Synthesis of integrated primary production in the arctic ocean: Ii. in situ and remotely  
55 sensed estimates. *Progress in Oceanography* 110, 107–125.  
56

- 1  
2  
3  
4 Juhls, B., Matsuoka, A., Lizotte, M., B'ecu, G., Overduin, P., El Kassar, J., Devred, E., Doxaran,  
5 D., Ferland, J., Forget, M., et al., 2022. Seasonal dynamics of dissolved organic matter in  
6 the Mackenzie delta, Canadian arctic waters: Implications for ocean colour remote  
7 sensing. *Remote Sensing of Environment* 283, 113327.  
8  
9  
10 Lizotte, M., Juhls, B., Matsuoka, A., Massicotte, P., M'evel, G., Anikina, D.O.J., Antonova, S.,  
11 B'ecu, G., B'eguvin, M., B'elanger, S., et al., 2023. Nunataryuk field campaigns:  
12 Understanding the origin and fate of terrestrial organic matter in the coastal waters of  
13 the mackenzie delta region. *Earth System Science Data* 15, 1617–1653.  
14  
15  
16 Massicotte, P., Amon, R.M., Antoine, D., Archambault, P., Balzano, S., B'elanger, S., Benner, R.,  
17 Boeuf, D., Bricaud, A., Bruyant, F., et al., 2021. The MALINA oceanographic expedition:  
18 how do changes in ice cover, permafrost and UV radiation impact biodiversity and  
19 biogeochemical fluxes in the arctic ocean? *Earth System Science Data* 13, 1561–1592.  
20  
21  
22  
23 Matsuoka, A., Babin, M., Vonk, J.E., 2022. Decadal trends in the release of terrigenous organic  
24 carbon to the Mackenzie delta (Canadian arctic) using satellite ocean color data (1998–  
25 2019). *Remote Sensing of Environment* 283, 113322.  
26  
27  
28 McClelland, J., Tank, S., Spencer, R., Shiklomanov, A., Zolkos, S., Holmes, R., 2023. Arctic great  
29 rivers observatory. Data retrieved from Arctic Great Rivers Observatory. Discharge  
30 Dataset, Version 20230630. <https://www.arcticrivers.org/data>.  
31  
32  
33 Miner, K.R., Turetsky, M.R., Malina, E., Bartsch, A., Tamminen, J., McGuire, A.D., Fix, A.,  
34 Sweeney, C., Elder, C.D., Miller, C.E., 2022.  
35 Permafrost carbon emissions in a changing arctic. *Nature Reviews Earth and*  
36 *Environment* 3, 55–67.  
37  
38  
39 Muggeo, V.M., 2003. Estimating regression models with unknown breakpoints. *Statistics in*  
40 *medicine* 22, 3055–3071.  
41  
42 Muñoz-Sabater, J., Dutra, E., Agust'ı-Panareda, A., Albergel, C., Arduini, G., Balsamo, G.,  
43 Boussetta, S., Choulga, M., Harrigan, S., Hersbach, H., et al., 2021. Era5-land: A state-of-  
44 the-art global reanalysis dataset for land applications. *Earth System Science Data* 13,  
45 4349–4383.  
46  
47  
48 Muñoz Sabater, J. (2019): ERA5-Land monthly averaged data from 1950 to present.  
49 Copernicus Climate Change Service (C3S) Climate Data Store (CDS). DOI:  
50 10.24381/cds.68d2bb30 (Accessed on 07-SEP-2023)  
51  
52  
53 Nitze, I., Cooley, S.W., Duguay, C.R., Jones, B.M., Grosse, G., 2020. The catastrophic  
54 thermokarst lake drainage events of 2018 in northwestern Alaska: fast-forward into the  
55 future. *The Cryosphere* 14, 4279–4297.  
56  
57  
58

- 1  
2  
3  
4 Ody, A., Doxaran, D., Verney, R., Bourrin, F., Morin, G.P., Pairaud, I., Gangloff, A., 2022. Ocean  
5 color remote sensing of suspended sediments along a continuum from rivers to river  
6 plumes: Concentration, transport, fluxes and dynamics. *Remote Sensing* 14, 2026.  
7  
8  
9 Poërtner, H.O., Roberts, D.C., Adams, H., Adler, C., Aldunce, P., Ali, E., Begum, R.A., Betts, R.,  
10 Kerr, R.B., Biesbroek, R., et al., 2022. *Climate change 2022: Impacts, adaptation and*  
11 *vulnerability*. IPCC Geneva, Switzerland.  
12  
13  
14 Spreen, G., Kaleschke, L., Heygster, G., 2008. Sea ice remote sensing using AMSR-e 89-ghz  
15 channels. *Journal of Geophysical Research: Oceans* 113.  
16  
17 Vigier, N., Bourdon, B., Turner, S., Allégre, C.J., 2001. Erosion timescales derived from u-  
18 decay series measurements in rivers. *Earth and Planetary Science Letters* 193, 549–563.  
19  
20 Wagner, A., Lohmann, G., Prange, M., 2011. Arctic river discharge trends since 7 ka bp. *Global*  
21 *and Planetary Change* 79, 48–60.  
22  
23  
24 Wang, M., Shi, W., 2007. The nir-swir combined atmospheric correction approach for modis  
25 ocean color data processing. *Optics express* 15, 15722– 15733.  
26  
27 Webb, E.E., Liljedahl, A.K., 2023. Diminishing lake area across the northern permafrost  
28 zone. *Nature Geoscience* 16, 202–209.  
29  
30  
31 Wegner, C., Hölemann, J.A., Dmitrenko, I., Kirillov, S., Kassens, H., 2005. Seasonal variations  
32 in arctic sediment dynamics—evidence from 1-year records in the Laptev sea (Siberian  
33 arctic). *Global and Planetary Change* 48, 126–140.  
34  
35 Winkelbauer, S., Mayer, M., Seitner, V., Zsoter, E., Zuo, H., Haimberger, L., 2022. Diagnostic  
36 evaluation of river discharge into the arctic ocean and its impact on oceanic volume  
37 transports. *Hydrology and Earth System Sciences* 26, 279–304.  
38  
39 Woo, M.K., Thorne, R., 2003. Streamflow in the Mackenzie basin, Canada. *Arctic*, 328–340.  
40  
41 Yang, D., Shi, X., Marsh, P., 2015. Variability and extreme of Mackenzie river daily discharge  
42 during 1973–2011. *Quaternary International* 380, 159–168.  
43  
44  
45 Zolkos, S., Zhulidov, A.V., Gurtovaya, T.Y., Gordeev, V.V., Berdnikov, S., Pavlova, N., Kalko, E.A.,  
46 Kuklina, Y.A., Zhulidov, D.A., Kosmenko, L.S., et al., 2022. Multidecadal declines in  
47 particulate mercury and sediment export from Russian rivers in the pan-arctic basin.  
48 *Proceedings of the National Academy of Sciences* 119, e2119857119.  
49  
50  
51  
52  
53  
54  
55  
56  
57  
58

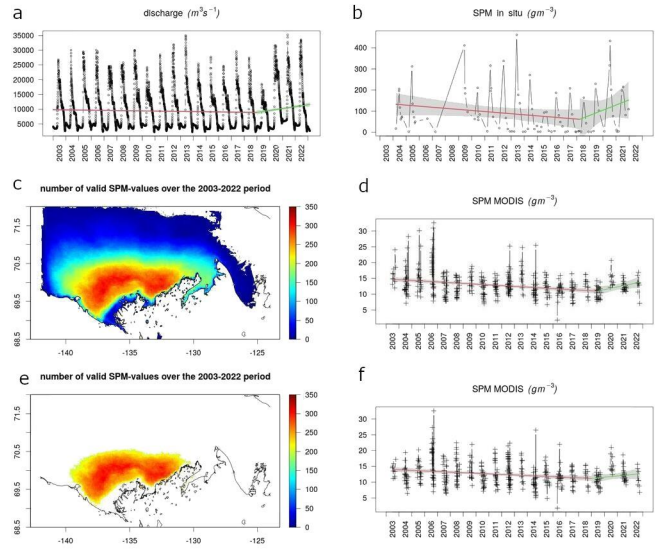


1  
2  
3  
4  
5  
6  
7  
8  
9  
10  
11  
12  
13  
14  
15  
16  
17  
18  
19  
20  
21  
22  
23  
24  
25  
26  
27  
28  
29  
30  
31  
32  
33  
34  
35  
36  
37  
38  
39  
40  
41  
42  
43  
44  
45  
46  
47  
48  
49  
50  
51  
52  
53  
54  
55  
56  
57  
58  
59  
60  
61  
62  
63  
64  
65

1 Graphical Abstract

2 **Variations of suspended particulate matter concentrations of the Mackenzie River**  
 3 **plume (Beaufort Sea, Arctic Ocean) over the last two decades**

4 Anastasia Tarasenko, David Doxaran, Bernard Gentili



5  
6

1  
2  
3  
4  
5  
6  
7  
8  
9  
10  
11  
12  
13  
14  
15  
16  
17  
18  
19  
20  
21  
22  
23  
24  
25  
26  
27  
28  
29  
30  
31  
32  
33  
34  
35  
36  
37  
38  
39  
40  
41  
42  
43  
44  
45  
46  
47  
48  
49  
50  
51  
52  
53  
54  
55  
56  
57  
58  
59  
60  
61  
62  
63  
64  
65

## 7 Highlights

### 8 **Variations of suspended particulate matter concentrations of the Mackenzie River** 9 **plume (Beaufort Sea, Arctic Ocean) over the last two decades**

10 Anastasia Tarasenko, David Doxaran, Bernard Gentili

- 11 • Interannual variations of suspended particulate matter (SPM) in coastal waters  
12 influenced by the Mackenzie River were investigated over the last 20 years (2003-  
13 2022) using MODIS/Aqua satellite data
- 14 • The offshore SPM variations are related to the Mackenzie River hydrological regime,  
15 air temperature, amount of snow, and permafrost state over its draining basin
- 16 • Over the last twenty years, a statistically significant negative trend was highlighted  
17 over the period 2003-2018 for both SPM and river discharge, with a positive trend  
18 starting from 2019 up to present

1  
2  
3  
4  
5 19 Variations of suspended particulate matter concentrations of  
6 20 the Mackenzie River plume (Beaufort Sea, Arctic Ocean) over  
7  
8 21 the last two decades  
9

10 22  
11 23 Anastasia Tarasenko<sup>a</sup>, David Doxaran<sup>a</sup>, Bernard Gentili<sup>a</sup>  
12

13 24 <sup>a</sup>Laboratoire d'Océanographie de Villefranche UMR 7093 CNRS Sorbonne Université 06230 Villefranche-sur-  
14 25 Mer France  
15  
16  
17

18 26  
19  
20 27 **Abstract**

21 28 This work addresses the last 20 years' evolution of the suspended particulate matter (SPM)  
22 29 concentrations in the Beaufort Sea (Canadian Arctic Ocean) directly influenced by the Mackenzie  
23 30 River discharge. The SPM variations in the coastal zone are highlighted and related to the freshwater  
24 31 and solid discharges of the river measured in situ at the Arctic Red River station (150 km upstream  
25 32 of the river delta). The correlation between the variations of the river discharge and SPM  
26 33 concentration within the surface layer of the coastal waters is obvious. Rather unexpectedly, both  
27 34 have been slightly but significantly decreasing from 2003 to 2018-2019 and started to increase very  
28 35 recently (2019-2022). This change of regime could be explained by changing winter precipitation  
29 36 and groundwater distribution, progressively accumulating sediments within the thawing  
30 37 permafrost layer and its recent release into the groundwater together with thermokarst lakes' rapid  
31 38 drainage.  
32  
33  
34

35 39 *Keywords:* suspended particulate matter, ocean optics, Arctic Ocean,  
36 40 MODIS  
37  
38  
39 41

40  
41 42 **1. Introduction**

42  
43 43 Climate change occurs faster in polar regions than at lower latitudes Arias et al. (2021).  
44 44 Global warming is usually associated in high latitudes with rising air temperature,  
45 45 precipitations, and permafrost thaw Miner et al. (2022); Pörtner et al. (2022).  
46 46 Consequently, the freshwater discharged by rivers into the Arctic Ocean is expected to  
47 47 increase, so as the discharge of terrestrial substances with enhanced erosion along  
48 48 drainage basins Doxaran et al. (2015); Matsuoka et al. (2022); Juhls et al. (2022). This  
49 49 would result in increasing water turbidity in coastal areas directly affected by river inputs  
50 50 but also boosted primary production due to higher nutrient loads and reduced sea ice cover  
51 51 (i.e., increasing solar light within the water column).  
52  
53  
54  
55  
56  
57  
58

1  
2  
3  
4 52 The Mackenzie River is the fourth largest Arctic river in terms of river discharge (7% of  
5 53 freshwater inflow to the Arctic Ocean) and is the primary source of sediment discharge  
6 54 Carson et al. (1998); Wagner et al. (2011); Yang et al. (2015), so the changes in the  
7 55 Mackenzie River regime will have a significant impact on the whole Arctic region Juhls et al.  
8 56 (2022). The Mackenzie has a prominent seasonal cycle with winter lows and a summer  
9 57 maximum of river discharge, which is related to the water cycle over its large basin with its  
10 58 75% permafrost area and the importance of snowmelt in spring Yang et al. (2015); Grotheer  
11 59 et al. (2020). The delta of the Mackenzie River is a complex area where the freshwater  
12 60 massively inflows into the southern Beaufort Sea, highly impacted by a long presence of sea  
13 61 ice. The southern Beaufort Sea is frozen most part of the year; the polynia between the fast  
14 62 ice of the delta starts opening in May, then the water surface stays mostly icefree from July  
15 63 to October. Over the last two decades, the sea ice conditions have become softer, and the sea  
16 64 ice concentration (SIC) has diminished by -4-8% per decade from 2003 to 2019 Hilborn  
17 65 and Devred (2022).

23 66 The open discussion of the Mackenzie River regime and its adaptation to climate change  
24 67 depends on the studied period Woo and Thorne (2003); Doxaran et al. (2015); Yang et al.  
25 68 (2015); Matsuoka et al. (2022); Zolkos et al. (2022). Doxaran et al. 2015 claimed a 22%  
26 69 increase of the river discharge from 2003 to 2013. Yang et al. 2015 showed that over the  
27 70 1973-2011 period, the positive linear trend for the Mackenzie discharge was very weak ( $y =$   
28 71  $17.21x + 8947.4$ ), and Woo and Thorne 2003 found no significant trend for the annual  
29 72 discharge over the period 1968-1999, nor did Matsuoka et al. 2022 for the 1992-2018  
30 73 period. Meanwhile, several studies agreed that the yearly amount of river discharge has  
31 74 changed its seasonal distribution: cold season discharge becomes slightly higher, but spring  
32 75 flows are lower (as higher air temperatures shift the snowmelt earlier) Woo and Thorne  
33 76 (2003); Yang et al. (2015). The question of the river water discharge, thus, should be  
34 77 regularly reevaluated.

39 78 In such a remote and changing environment, satellite observations have been proven to  
40 79 be an efficient tool to monitor the evolution of Arctic coastal zones, and compensate the  
41 80 lack of field measurements Doxaran et al. (2012); Hill et al. (2013); Juhls et al. (2022). SPM  
42 81 field measurements, although extremely valuable, are usually too sparse for the long-term  
43 82 variability analysis, as most of them are associated with specific summer expeditions (e.g.  
44 83 the recent MALINA Massicotte et al. (2021) and Nunataryuk Lizotte et al. (2023) field  
45 84 campaigns). Overall, during the ice-free season, satellite-derived suspended particulate  
46 85 matter (SPM) concentrations typically vary from  $30 \text{ g/m}^3$  in the delta region to  $0.5 \text{ g/m}^3$   
47 86 offshore over the Canada Basin Hilborn and Devred (2022).

51 87 Several studies analyzed satellite-derived SPM concentration variability in the southern  
52 88 Beaufort Sea for long time periods (over 10 years), and their results are rather  
53 89 controversial. From 2003 to 2013, Doxaran et al. 2015 found a linear trend with a significant  
54 90 increase in monthly- averaged SPM concentrations at the mouth of Mackenzie River (+46%  
55 91 in 10 years over the river mouth area and +71% in the river delta south to  $70^\circ\text{N}$ ). Hilborn

and Devred 2022 applied *self-organizing maps* method to identify six different regions in the eastern Beaufort Sea using 17 years of MODIS (Moderate Resolution Imaging Spectroradiometer) data and found only one statistically significant trend (negative) for the annual SPM concentration in the deepwater Canada basin area, far offshore the Mackenzie delta. At the same time, Matsuoka et al. 2022 showed a statistically significant increase of dissolved and particulate organic matter concentrations (but not fluxes) in late summer: 0.019  $g/m^3$  per year and 0.069  $g/m^3$  per year, accordingly).

The present study is a continuation of Doxaran et al. 2015, where we analyze the evolution of the SPM concentration in the Beaufort Sea directly influenced by the discharge of the Mackenzie River over the last two decades (2003-2022), using the methodology developed by Doxaran et al. (2012, 2015), this time excluding the complex river delta zone.

## 2. Materials and Methods

Fig. 1a shows the limits of the study area (yellow rectangular) on a quasitrue color daily MODIS composite for August 8, 2016. In this image, the SPM-rich Mackenzie River plume propagates along the coast and northward, partly into the MIZ (marginal ice zone). The variations of SPM concentrations (Fig. 1b) from the delta to offshore waters are obvious, which highlights complex processes along this land-sea interface. The field and satellite datasets used in this study, so as the methods used to retrieve and analyze time series of river discharge and SPM concentrations, are detailed hereafter.

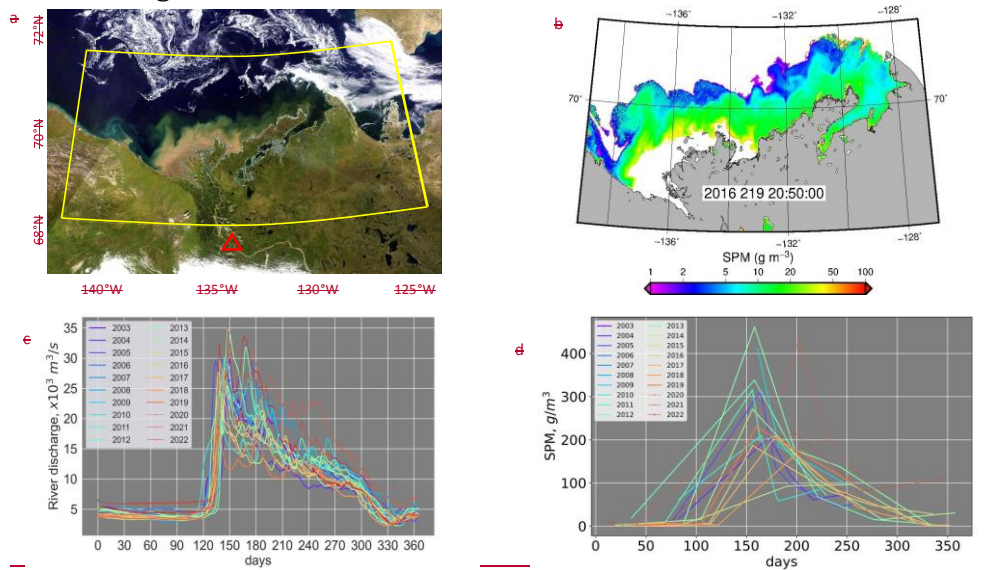


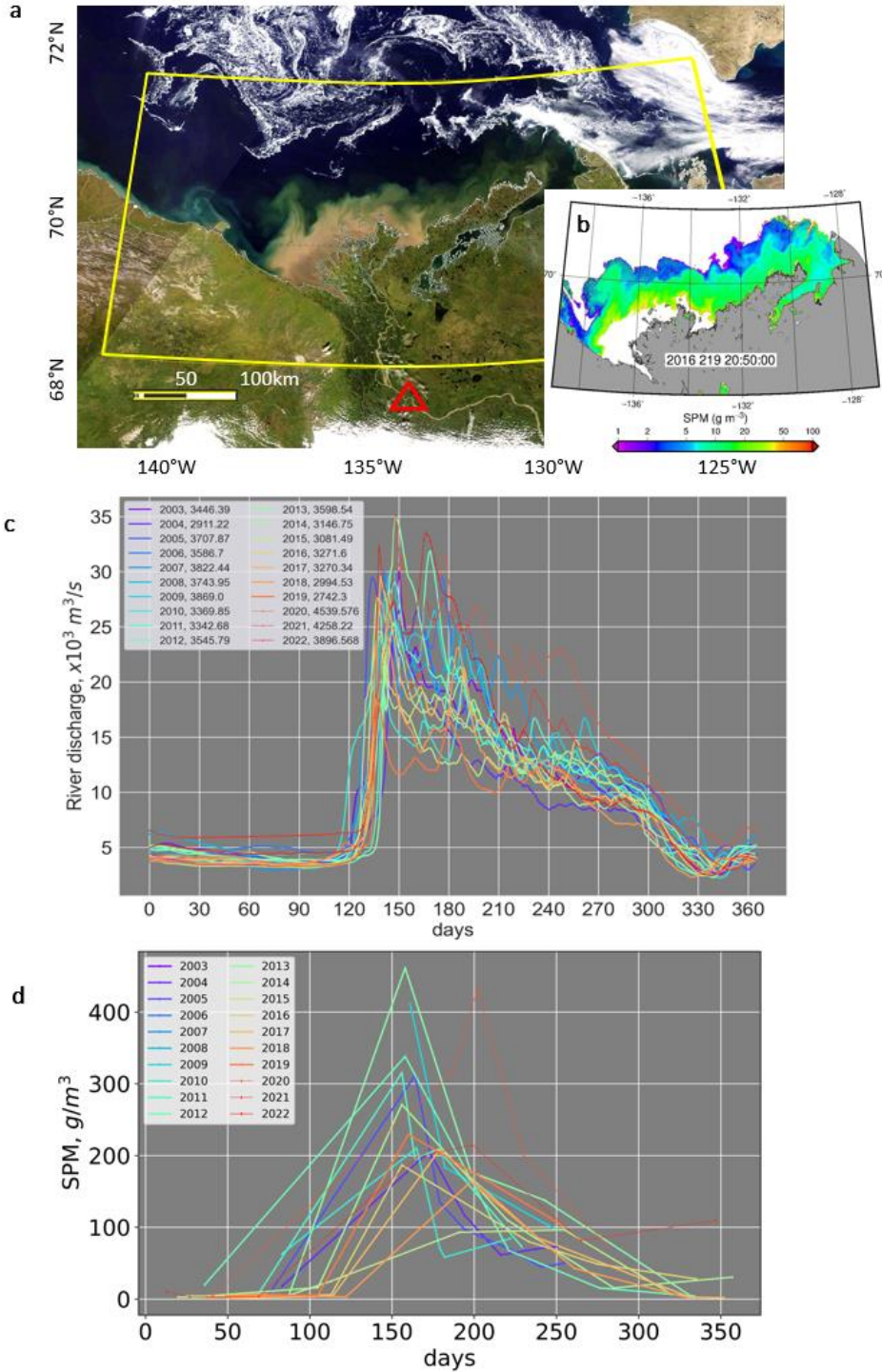
Figure 1: (a) MODIS image (August 6, 2016) locating the Arctic Red River gauge station (Tsiigehtchic) where in situ measurements are carried out (red triangle) and the coastal waters studied using satellite data (yellow rectangle); (b) SPM concentrations: Interannual variations of liquid discharge (c) and SPM concentrations (d) at the Arctic Red River station. The inserted SPM color map shows the result of MODIS satellite data processing

1  
2  
3  
4  
5  
6  
7  
8  
9  
10  
11  
12  
13  
14  
15  
16  
17  
18  
19  
20  
21  
22  
23  
24  
25  
26  
27  
28  
29  
30  
31  
32  
33  
34  
35  
36  
37  
38  
39  
40  
41  
42  
43  
44  
45  
46  
47  
48  
49  
50  
51  
52  
53  
54  
55  
56  
57  
58  
59  
60  
61  
62  
63  
64  
65

## 2.1. Field data sets

In situ measurements of the river water discharge (2003-2022) were provided by the Water Survey of Canada via the ArcticGRO project McClelland et al. (2023) at the Arctic Red River gauge station (station ID: 10LC014, 67.45°N 133.74°W, red triangle in Fig.1a). River discharge measurements,  $Q$ , are available daily (Fig.1c). The measurements of suspended matter are distributed by the ArcticGRO as *total suspended solids (TSS)* concentrations, which is the same as SPM, so hereafter we will refer to in situ TSS as the *SPM<sub>insitu</sub>*. The *SPM<sub>insitu</sub>* data were collected at most once per month, but not during all months (on average, 4 to 6 measurements per year, Fig.1d). Over the studied period, some years are poorly represented (one measurement per year in 2003, 2006, and 2007; no SPM measurement in 2008). The lack of SPM in situ data implies the necessity to use satellite data.

The ArcticGRO in situ datasets pass the quality control procedure and indicate less reliable measurements as "provisional data". Over the 2003-2022 period, it corresponds to river discharge data in 2020-2022 and *SPM<sub>insitu</sub>* data in 2019-2022 (shown with thinner lines in Fig.1c, d).



135  
136 **Figure 1: (a) MODIS image (August 6, 2016) locating the Arctic Red River gauge station (Tsiigehtchic) where**  
137 **in situ measurements are carried out (red triangle) and the coastal waters studied using satellite data (yellow**  
138 **rectangle); (b) SPM concentrations: Interannual variations of water discharge (the year of measurement and**

1  
2  
3  
4 139 [the annual cumulative sum of discharge is indicated in legend\), \(c\) and SPM concentrations \(d\) at the Arctic](#)  
5 140 [Red River station. The inserted SPM color map shows the result of MODIS satellite data processing](#)  
6  
7 141

## 9 142 2.2. Ocean color satellite data

10 143 As in Doxaran et al. 2015, a single satellite sensor (MODIS/Aqua) was considered for  
11 144 this study in order to avoid any bias between different sensor products when detecting  
12 145 temporal trends. Since 2003, MODIS provides high-quality ocean color observations at a  
13 146 good temporal resolution: several images per day of the study area during the Arctic  
14 147 summer months Doxaran et al. (2012, 2015); Hilborn and Devred (2022); Matsuoka et al.  
15 148 (2022). The region of interest was defined as 68.5°N-72°N, 142°W - 124°W (yellow  
16 149 rectangle in Fig.1a). The initial dataset contained 10608 swaths collected between May 1  
17 150 and October 31 each year over the 2003-2022 period.

21 151 *Processing of satellite data.* MODIS L1A satellite data were processed using the SeaWiFS  
22 152 Data Analysis System (SeaDAS 8.1.0) software (<http://seadas.gsfc.nasa.gov/>) and its l2gen  
23 153 function. The atmospheric correction was performed using the NIR-SWIR algorithm of  
24 154 Wang and Shi 2007); this method was proved to be the most appropriate for the highly  
25 155 turbid waters at the mouth of the Mackenzie River to the less turbid waters offshore  
26 156 Doxaran et al. (2012).

29 157 SeaDAS l2gen flags were used to mask clouds and glint. In the work of Doxaran et al.  
30 158 2015, two techniques were used to mask clouds: the default one in the coastal waters and  
31 159 an increased cloud albedo threshold value (0.4 instead of 0.027) over the specific area of  
32 160 the river delta zone to avoid masking the highly turbid water pixels. This procedure was  
33 161 time-consuming and required an additional inspection of every image in the river delta  
34 162 zone. Here, the cloud-masking method preconized by Ody et al. 2022 for river mouths was  
35 163 used to process each satellite image only once: the 2130 nm shortwave-infrared waveband  
36 164 was used with a cloud threshold of 0.018. The sea ice mask was computed from daily sea  
37 165 ice concentration (SIC) data at 3.125°spatial resolution distributed by the University of  
38 166 Bremen Spreen et al. (2008). This dataset contains AMRS-E and AMSR2 (Advanced  
39 167 Microwave Scanning Radiometer -for Eos and -2) images. Due to several gaps in data  
40 168 acquisition over the 2003-2022 time period, the dataset was completed with the sea ice  
41 169 concentration from the SSMIS (Special Sensor Microwave Imager/Sounder) instrument.  
42 170 The ice mask was created using the SIC above 0%.

48 171 All satellite data (Rayleigh-corrected reflectances and masks) were reprojected on a  
49 172 regular 250 m grid. The following criteria were then applied to exclude potentially  
50 173 contaminated images:

- 53 174 • the number of valid pixels should exceed 15% of the marine area of the study area in  
54 175 the downloaded MODIS image;



- the distance between the central point of the study area and that of the MODIS image should be less than 1000 km to avoid aberrations on the border of the image;
- only areas with a zenith solar angle lower than 74° were conserved.

This automatic filtering reduced the MODIS collection to 700 images. Finally, all images were inspected visually to filter out the remaining contaminated images because of not detected MIZ, clouds or cloud shadows, etc.; 651 MODIS images remained after this last quality check step.

The SPM concentrations were computed from the ratio (in %) between the remote sensing reflectance signals,  $R_{rs}$  (in  $sr^{-1}$ ) in the near-infrared and green wavebands using the set of relationships established based on field measurements Doxaran et al. (2012, 2015):

$$SPM_{sat} = 0.8386 \times R_{RS}(748 : 555) \quad (1)$$

if  $R_{RS}(748 : 555) < 87\%$

$$SPM_{sat} = 70 + 0.1416 \times R_{RS}(748 : 555) + 2.9541 \times e^{0.2092 \times (R_{RS}(748:555) - 87)} \quad (2) \text{ if } 87\% \leq R_{RS}(748 : 555) \leq 94\%$$

$$SPM_{sat} = 3.922 \times R_{RS}(748 : 555) - 285.4 \quad (3)$$

if  $94\% < R_{RS}(748 : 555)$ , where  $SPM_{sat}$  is the SPM concentration in  $g/m^3$  and  $R_{RS}(748 : 555)$  is the ratio of remote-sensing reflectances at 748 and 555 nm.

Negative  $R_{RS}(555)$  and  $R_{RS}(748)$  values were discarded before computing SPM, as well as computed SPM concentrations higher than 1000  $g/m^3$ , to remove atmospheric correction failures and residual contaminations (typically encountered along borders of clouds or sea ice).

The processed SPM images were averaged as daily, monthly, and yearly composites as simple mean averages for every pixel. Only daily composites and their mean values were used further, as monthly composites were sometimes computed using only 1 to 3 cloud-free images, which is not representative of mean monthly concentrations.

### 2.3. Reanalysis data

A dataset from ERA5 Land reanalysis was extracted to better understand how environmental factors did impact the Mackenzie River discharge and SPM concentrations in the adjacent coastal waters. This dataset was selected as the most suitable tool for the studies of river discharge variability Winkelbauer et al. (2022). ERA5 Land has a monthly temporal resolution and 9-km spatial resolution and is provided by Copernicus data center [MuñozMuñoz-Sabater et al. \(2021\)](#). The area of extraction approximately corresponds to the Mackenzie drainage basin (52-70°N, 100-140°W). The following parameters were used: river runoff (ro), surface river runoff (sro), evaporation (e), total precipitation (tp), snow

1  
2  
3  
4 210 depth (sd), and air temperature at 2m (t2m), (see ~~de-detailed description at~~  
5 211 <https://confluence.ecmwf.int/display/CKB/ERA5-Land%3A+data+document> The  
6 212 [Pearson correlation matrix for the mean annual values of all described parameters](https://confluence.ecmwf.int/display/CKB/ERA5-Land%3A+data+document)  
7 213 (Fig.A.3).

8 214 ~~tailed description at~~  
9 215 [https://confluence.ecmwf.int/display/CKB/ERA5-](https://confluence.ecmwf.int/display/CKB/ERA5-Land%3A+data+document)  
10 216 [Land%3A+data+document](https://confluence.ecmwf.int/display/CKB/ERA5-Land%3A+data+document) The similarity between the ERA5-LAND  
11 217 river runoff and the Arctic GRO river discharge are shown in the  
12 218 Supplementary Information section (Fig.), as well as a correlation  
13 219 matrix for the mean annual values of all described parameters  
14 220 (Fig.S12).

15 221 To include a possible effect of storms on the SPM concentrations, we added to the  
16 222 analysis the wind data from ERA5 (marine area similar to that chosen for the MODIS study  
17 223 box). The Pearson correlation matrix (where the yearly parameters are compared) contains  
18 224 an additional parameter "the number of days of storms per year" (*ndays\_storm* in Fig. A.3).  
19 225 The day was considered stormy if over the study area there was a wind vector with a wind  
20 226 speed over 15 m/s.

#### 21 227 2.4. Temporal variability

22 228 As previous works have shown, the linear regression model provides relatively little  
23 229 information on interannual variability of river water discharge and related parameters,  
24 230 such as SPM, because, over the long term, the discharge appears as stable Yang et al. (2015);  
25 231 Matsuoka et al. (2022). Over the last 20 years, the linear trend for the in situ Mackenzie  
26 232 discharge time series calculated with the Ordinary Least Squares (OLS) model is  $y =$   
27 233  $17.1x + 9554$  with a standard error (SE) of  $63.6 \text{ m}^3/\text{s}$ , and confidence intervals (CI)  $[0.025$   
28 234  $0.975]$  equal to  $-107.5$  and  $141.7 \text{ m}^3/\text{s}$  for the coefficient term. Although these results are  
29 235 very close to that of Yang et al. 2015, the statistical metrics confirm that the OLS model is  
30 236 not suitable for the analysis in this case.

31 237 For this reason, we used an estimating regression model with unknown break-points,  
32 238 which allows describing several temporal trends Muggeo (2003). To apply this model to  
33 239 our datasets, we used the *segmented* function in the R package *segmented*.

34 240 To compute the trends, the in situ data time series of daily river discharge ( $Q_{insitu}$ ) and  
35 241 SPM concentration ( $SPM_{insitu}$ ) described above were used (Fig.2a, b). For the satellite data,  
36 242 the spatial sparsity of observations was taken into account. Thus, to obtain  $SPM_{sat}$  time  
37 243 series, we calculated: • one daily spatial mean SPM value for all available SPM pixels over  
38 244 the study area, which resulted in  $SPM_{sat}$  time series (Fig.2 c-d); • one daily spatial mean SPM  
39 245 value for the area with the highest data density (where valid satellite pixels appear more  
40 246 than 200 times over the 2003-2022 period), which resulted in  $SPM_{sat200}$  (Fig.2 e-f)

1  
2  
3  
4 247 Then the segmented regression analysis technique was applied to all time series:  $Q_{insitu}$ ,  
5  
6 248  $SPM_{insitu}$ ,  $SPM_{sat}$ , and  $SPM_{sat200}$ . After several tests, the most statistically significant results  
7 249 were obtained with one breaking point and two segment slopes. The following statistical  
8  
9 250 parameters were computed for each segment: estimated coefficient of linear regression  
10 251 (Est.), standard error, lower and upper 95% confidence intervals (CI(95%).l, CI(95%).u,  
11 252 respectively) (Tab.1).  
12  
13

### 14 253 3. Results and Discussion

15  
16 254 The seasonal cycles of both the river discharge,  $Q$ , and  $SPM_{insitu}$  are very pronounced,  
17 255 with high summer and low winter values (Fig.1c,d). These parameters also have a strong  
18 256 interannual variability. During the 2003-2022 period, the river discharge varied from  
19 257  $2.2 \times 10^3 \text{ m}^3/\text{s}$  (winter) to  $35.2 \times 10^3 \text{ m}^3/\text{s}$  (summer), with a mean value of  $9.5 \pm 6.8 \times 10^3 \text{ m}^3/\text{s}$ .  
20  
21 258 Typically, the discharge increases very rapidly in 2 weeks from 5 to  $25 \times 10^3 \text{ m}^3/\text{s}$  in late May,  
22 259 when the main summer peak occurs, then slowly decreases to its winter values by  
23  
24 260 November.  
25

26 261 The years 2013 and 2021 were exceptional with extreme *yearly maxima* of river  
27 262 discharge over  $35 \times 10^3 \text{ m}^3/\text{s}$  on May 28 (both), while the lowest yearly maximum river  
28 263 discharge,  $18 \times 10^3 \text{ m}^3/\text{s}$ , was registered on May 18, 2019. Previously, Yang et al. 2015 also  
29 264 observed similar prominent interannual variations in the river discharge during the  
30 265 summer (e.g., in 1992 and 1995 for the 1972-2011 period). They concluded that a negative  
31 266 anomaly in precipitation-evaporation balance over the river basin in summer (hot and dry  
32 267 weather) usually results in a lower discharge the next year with an earlier maximum, while  
33 268 the opposite (cold and wet) weather is responsible for a higher discharge. This statement  
34 269 does not explain the extreme peak of discharge recorded in 2013: in 2012 the summer was  
35 270 "hot and dry", so 2013 should have been a year of extremely low summer river discharge.  
36  
37 271 Overall, calculated correlations between in situ river discharge and ERA5 Land total  
38 272 precipitation, as well as air temperature were weak (0.36 and -0.23, respectively).  
39  
40 273

41 274 However, the river discharge is well correlated with snow depth  
42 275 cover  
43 276 (correlation coefficient between  $Q_{insitu}$  and  $sd$  is 0.67): the 2011-12 and ~~2012-13~~ 2012-13  
44 277 winters were ~~very~~ snowy (+10% and +3%  $sd$  anomaly compared to 20years median  
45 278 values), as well as the 2020 winter (+7%  $sd$  anomaly), but 2018-19 snow cover was weak  
46 279 (-7%  $sd$  anomaly). Interestingly, in 2013 the yearly means of river discharge and air  
47 280 temperature were close to their 20years median values, indicating the overall stability of  
48 281 the system during this period.  
49  
50  
51  
52

53 281 The river discharge regime in 2006-2008 and 2012 was special with two summer  $Q$   
54 282 maxima, the first one in late May and the second between the end of June and mid-July. The  
55 283 reason for this change in river regime might be related to the precipitation seasonal pattern  
56 284 and the river ice opening (several ice jams crushes, creating the second peak). To investigate  
57  
58

1  
2  
3  
4 285 these particularities, a higher temporal resolution reanalysis data should be used. We also  
5  
6 286 observe local maxima (values higher than the previous year) in  $SPM_{sat}$  in 2006, 2008, and  
7 287 2012.

8 288 As explained in section 2.4, the OSL model does not highlight a statistically significant  
9  
10 289 trend in the river discharge time series, but the *segmented* model does. Fig.2 and Table 1  
11 290 present the results of calculated segmented regressions, where the river discharge and SPM  
12 291 concentrations demonstrate very similar trends: a negative trend from 2003 to 2018, then  
13 292 a recent positive trend from 2019 (2018 for  $SPM_{insitu}$ ) to 2022 (Fig.2). Based on the  
14 293 confidence intervals, we conclude that negative trends for  $slope1_Q$ ,  $slope1_{SPM_{sat}}$ , and  
15 294  $slope1_{SPM_{sat200}}$  are statistically significant (CIs [0.025 0.975] are all negative).

16 295 This negative trend of  $slope1_Q = -57.21x + const$  in river discharge for the 2003-2018  
17 296 period is opposite to that of Doxaran et al. 2015 for the 2003-2013 period, but the latter  
18 297 study slightly overestimated the river discharge in 2013 (as the data was not yet fully  
19 298 quality-checked) resulting in an erroneous positive (+22%) trend. As already mentioned,  
20 299 other studies, e.g. Yang et al. (2015); Matsuoka et al. (2022) which used an OSL model did  
21 300 not find any significant trend in the Mackenzie River discharge. The positive trend from  
22 301 2019 to the present,  $slope2_Q = 640.05x + const$ , although not statistically significant, can  
23 302 indicate a progressive increase in the minimum flow impacted by a "mobilization of ground  
24 303 waters" as discussed by Yang et al. 2015.

25 304 In situ data show that the SPM seasonal cycle generally follows the river discharge cycle,  
26 305 with the summer maxima in late May - beginning of June. The  $SPM_{sat}$  values vary from 0.8  
27 306 to  $461 \text{ g/m}^3$  with a median value of  $67.7 \pm 11 \text{ g/m}^3$ . The breakpoint of  $SPM_{insitu}$  trends is  
28 307 slightly shifted to 2018, and CIs contain zero, thus indicating that the *segmented* model is  
29 308 less reliable for this dataset. At the same time, the  $SPM_{insitu}$  time series has the fewest amount  
30 309 of data, which is not homogeneous in time and is mainly available in summer. It makes it  
31 310 more difficult to interpret with any statistical model.  $SPM_{sat}$  and  $SPM_{sat200}$  trend analyses  
32 311 show similar results: their negative  $slope1$  values and corresponding SE are close to each  
33 312 other, which gives confidence in the observed SPM negative trend. The positive trends  
34 313  $slope2_{sat}$  and  $slope2_{sat200}$  are not statistically significant, and their SEs are of the order of the  
35 314 estimated coefficient of linear regression (Tab.1). Nevertheless, this result is interesting for  
36 315 further discussion.

37 316 Over the 2003-2019 period, Hilborn and Devred 2022 obtained results in good  
38 317 agreement with a negative trend (although not significant) for SPM concentrations over the  
39 318 southern Beaufort Sea (from -0.16 to  $-0.46 \text{ g/m}^3$  per decade) except for the Mackenzie River  
40 319 delta, where they found an increase of SPM of  $0.36 \text{ g/m}^3$  per decade. The difference in  
41 320 negative coefficients' values obtained in the present study and that of Hilborn and Devred  
42 321 (2022) comes from (1) the difference of SPM-retrieval methods and different MODIS bands  
43 322 used; and (2) the regions: our study region of  $SPM_{sat200}$  corresponds to 3 regions over the  
44 323 shelf identified by Hilborn and Devred (2022).

1  
2  
3  
4 324 In the Mackenzie delta zone, Doxaran et al. 2015 also found a significant increase of SPM  
5 325 (+71% from 2003 to 2013) over the "Mackenzie River delta" region of Hilborn and Devred  
6 326 (2022). The delta zone seems to play an important role of "SPM filter" between the river  
7 327 and the coastal waters. Based on satellite observations, SPM apparently settles massively  
8 328 in this shallow area, resulting in the formation of temporary maximum turbidity zones  
9 329 where resuspension of bottom sediments may occur depending on the river discharge, tidal  
10 330 currents, and wind stress (Wegner et al., 2005; Grotheer et al., 2020). Observations at  
11 331 high spatial and temporal resolutions are required to further investigate SPM dynamics in  
12 332 this delta zone.

13  
14  
15  
16 333 However, how to explain the negative trends in both river discharge and SPM  
17 334 concentrations (in the riverbed and offshore the delta zone) derived from field and satellite  
18 335 observations over the 2003-2018 period? ~~The Based on the correlation matrix (Fig. A.3),~~  
19 336 ~~we recognize that the river runoff and, thus, river discharge variability depend mostly on~~  
20 337 ~~the amount of total precipitation (r = 0.7) and the snow depth (r = 0.63, which is another~~  
21 338 ~~estimate of solid precipitation in winter) parameters. This trivial conclusion leads us to a~~  
22 339 ~~simple suggestion that the Mackenzie River discharge slightly declined while the~~  
23 340 ~~precipitation pattern has changed over this period.~~

24  
25  
26  
27 341 As for the SPM, the recent study of Zolkos et al. 2022 reveals a similar decrease in SPM  
28 342 loads in most of the Russian Arctic-Siberian rivers between 1970 and 2010, and explains it  
29 343 by natural and anthropogenic factors. At the same time, the rivers' discharge (mean and  
30 344 peak values) The "natural factors" of sediments erosion over the river basin are the physical  
31 345 and chemical denudation. For the Mackenzie River, the physical denudation rates exceed  
32 346 the chemical denudation about several orders of time: mechanical denudation rate at the  
33 347 Arctic Great River was reported as 844 t \* km<sup>-2</sup> \* y<sup>-1</sup> in 1997, while the chemical  
34 348 weathering occurs at a rate of 25 mm\*ky<sup>-1</sup> with a transport time of 10-400 ky<sup>-1</sup> (Vigier et  
35 349 al. (2001); DePaolo et al. (2006)). On the order of two decades, it is, thus, physical or  
36 350 mechanical factors related to the river discharge and the atmospheric conditions in the  
37 351 delta-adjacent areas that control SPM concentrations. A simultaneous decline of Q *in situ*  
38 352 and SPM *in situ* in 2003-2018 means that the lower the river discharge, the less suspended  
39 353 particulate matter it transports.

40  
41  
42  
43  
44 354 Another source of variability for the "marine" SPM might be the wind mixing. The simple  
45 355 hypothesis proposes that the higher the wind speed, the more mixing occurs in a shallow  
46 356 area, which reduces the surface SPM concentrations. At the same time, an additional  
47 357 hypothesis may suggest that more mixing means more re-suspension of particulate matter  
48 358 from the bottom sediments (increasing the SPM concentration). To verify these  
49 359 controversial hypotheses, we must compare quasi simultaneous wind and SPM  
50 360 observations. In the framework of this study there is yet one fundamental limitation for  
51 361 this analysis due to the nature of ocean color data retrieval from satellite: the highest wind  
52 362 speed (and thus mixing events) will mostly occur under the cloud cover with the passage  
53 363 of cyclones, and SPM concentrations cannot be retrieved from ocean color satellite under  
54 364 such conditions (presence of clouds). We found a weak negative correlation (correlation  
55  
56  
57  
58

1  
2  
3  
4 365 coefficient is  $r=-0.19$ ) between the number of days of storm and annual cumulated SPM,  
5 366 which confirms the first simple hypothesis (more mixing, less SPM), but this question  
6 367 should be addressed additionally with other tools, like modeling.

7 368 There is yet a question about the recent positive trends in  $Q$  and SPM over the last 3-5  
8 369 years of observations. Although the trends are statistically not significant, can we suggest  
9 370 any important processes that might have impacted the river discharge and sedimentation  
10 371 transport recently?

11 372 The presence of permafrost over the river basin was considered  
12 373 mostly stable, so the link between the river discharge and SPM load is  
13 374 not straightforward. Zolkos et al. suggest that the decrease of SPM is  
14 375 due to the decrease of the sediments input “and/or increased  
15 376 sedimentation within the fluvial network”. Nonetheless, the Kolyma  
16 377 yearly SPM flux has doubled over the same period, which was  
17 378 associated with the geological stratification of more erodible  
18 379 quaternary sediments altering with ice. In the Canadian Arctic “where  
19 380 large areas are susceptible to hillslope thermokarst activity”, the  
20 381 permafrost thaw can induce the downstream redistribution of  
21 382 particular sediments over the next “centuries or millennial”. We might  
22 383 observe the effect of the sediment accumulation during a “precluding”  
23 384 for the groundwater’s contribution to general river discharge, as it  
24 385 prevented the water infiltration through the permafrost layer, but  
25 386 might have helped to create underground cavities filled with non-  
26 387 communication water reservoirs (Vigier et al. (2001)). With a  
27 388 progressive permafrost thawing and its recent release in SPM  
28 389 measurements.

29 390 The permafrost thaw likely controls as well the drainage of lakes located in the  
30 391 permafrost area Webb and Liljedahl (2023)., this neglected role might be re-evaluated.  
31 392 Matsuoka et al. 2022 observed an increase of thaw depth and precipitation, but a decrease  
32 393 in river discharge, which is probably explained by the contribution of ground waters, also  
33 394 suggested by Connolly et al. (2020). Finally, The permafrost thaw also likely affects  
34 395 the drainage of lakes located in the permafrost area Webb and Liljedahl (2023). A recent  
35 396 work of Nitze et al. 2020 described, e.g., a series of extremely quick thermokarst lakes drainage  
36 397 in 2018 in northwestern Alaska after the unprecedented warm (with air temperature close  
37 398 to 0°C) and wet winter of 2017-2018. This drainage “exceeded the average drainage rate by  
38 399 a factor of 10”, and is supposed to continue and increase the liquid and solid discharges of  
39 400 Arctic rivers. This situation suggests that in the Canadian Arctic, where “large areas are  
40 401 susceptible to hillslope thermokarst activity” (Zolkos et al. (2022)), the permafrost thawing  
41 402 will progressively change chemical denudation and induce the downstream redistribution  
42 403 of sediments over the next millennial(s).

43 404 Based on these results, we conclude that the following mechanism ex-  
44 405

Table 1: Statistics for the segmented linear regression analysis of in situ river discharge (Fig.2a) -  $slope_Q$ ; trends of  $SPM_{insitu}$ :  $slope_{insitu}$  (Fig.2b); trends of  $SPM_{sat}$  for all available points:  $slope_{sat}$  (Fig.2d); and trends for  $SPM_{sat}$  for the area with over 200 pixels available:  $slope_{sat200}$  (Fig.2f). Negative trend parameters are described with  $slope1$ , positive with  $slope2$

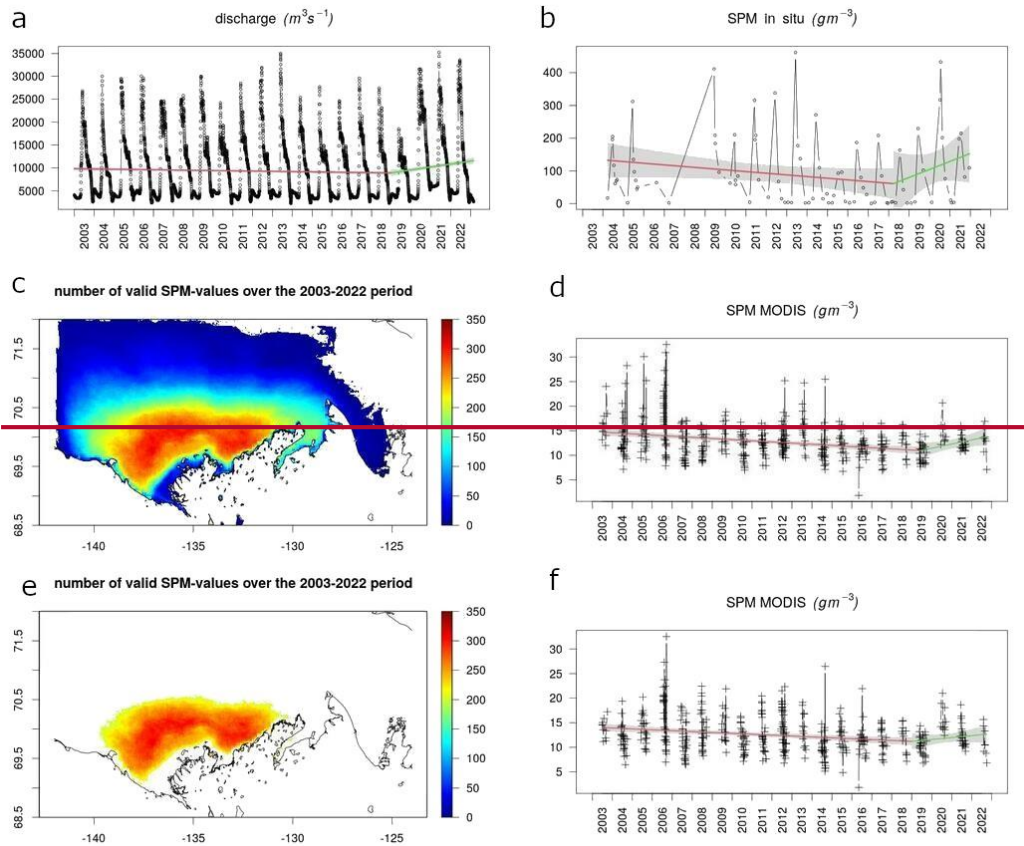
	Est.	Standard error	CI(95%).l	CI(95%).u
$slope1_Q$	-57.21	19.14	-94.73	-19.68
$slope2_Q$	640.05	142.91	359.88	920.19
$slope1_{insitu}$	-5.08	3.04	-11.13	0.96
$slope2_{insitu}$	24.46	21.86	-19.02	67.93
$slope1_{sat}$	-0.23	0.04	-0.32	-0.15
$slope2_{sat}$	0.84	0.43	-0.01	1.70
$slope1_{sat200}$	-0.18	0.04	-0.27	-0.09
$slope2_{sat200}$	0.39	0.40	-0.40	1.18

~~plains the observed negative trend in river discharge and SPM concentrations switched by a rapid positive trend: the progressive thaw of the permafrost helped to accumulate sediments in the ground inner impermeable layers up to the certain moment (appr. 2018), then these additional sediments arrived into the groundwater, and together with the drainage of lakes, the accumulated sediments started its quick release with groundwater into the main surface flow and the Beaufort Sea.~~

#### 4. Conclusion

Twenty years (2003-2022) of in situ measurements (river discharge and SPM concentration at the Arctic Red River station) and satellite-derived SPM concentrations were analyzed to describe the evolution of SPM inputs in the Beaufort Sea by the Mackenzie River and its impact on the adjacent coastal waters. Using the segmented regression model, we showed two opposite trends over the last 20 years for both the river freshwater discharge and SPM concentration. Over the studied period, we observe a statistically significant negative ~~trend~~trends from 2003 to 2018-2019, then a positive trend from 2019 to 2022 for both river discharge and SPM concentrations. Our results extend previous estimations of Doxaran et al. 2015 and tend to confirm other long-term observations showing a rather stable freshwater

442 discharge of the Mackenzie River, increasing SPM concentrations in the  
 443 delta zone and a significant decrease in SPM concentration in adjacent



444  
 445 Figure 2: Interannual variations of in situ and satellite data (river discharge and SPM) with their segmented  
 446 linear regression slopes (red and green colors show negative and positive regressions, respectively): (a) river  
 447 discharge  $Q_{in\ situ}$ , (b)  $SPM_{in\ situ}$  time series; (c) maximum number of valid  $SPM_{sat}$  pixels in 2003-2022 (d) satellite  
 448  $SPM_{sat}$  time series;  
 449 (e-f) similar to (c-d), but for the area with at least 200 valid pixels

450 coastal waters Feng et al. (2021); Hilborn and Devred (2022); Matsuoka et al. (2022).

451 We suggest that the observed variability indicates a ~~recent progressive accumulation of~~  
 452 ~~sediments during the permafrost thaw, its further release into the drainage system,~~  
 453 ~~Mackenzie flow, and finally into the Beaufort Sea since 2018. An important snow~~  
 454 ~~accumulation followed by a spring thawing with extreme air temperatures aggravates the~~  
 455 ~~drainage and sediment accumulation and release on the medium-term timescale.~~  
 456 ~~simultaneous decline of water discharge and, thus, suspended particulate matter transport~~  
 457 ~~due to changing precipitation pattern, especially the amount of snow over the river basin~~  
 458 ~~with a possible role of wind-induced mixing in the marine area. We also discuss long-term~~  
 459 ~~effects of climate change and permafrost thawing on the sediment transport rate in the~~  
 460 Mackenzie River.



These processes of SPM release into the Arctic Ocean should be studied next on a pan-Arctic scale: can we expect a similar behavior based on the regional variations of river discharges reported by ArcticGRO? A recent study of Zolkos et al. 2022 used only in situ data, and further analysis of SPM distribution into the Arctic Ocean with satellite data will be beneficial. Studying the seasonal variability for specific years (e.g., 2006-2008, 2012) is also required using higher resolution data, including satellite imagery, to better understand changing river regimes in Arctic regions.

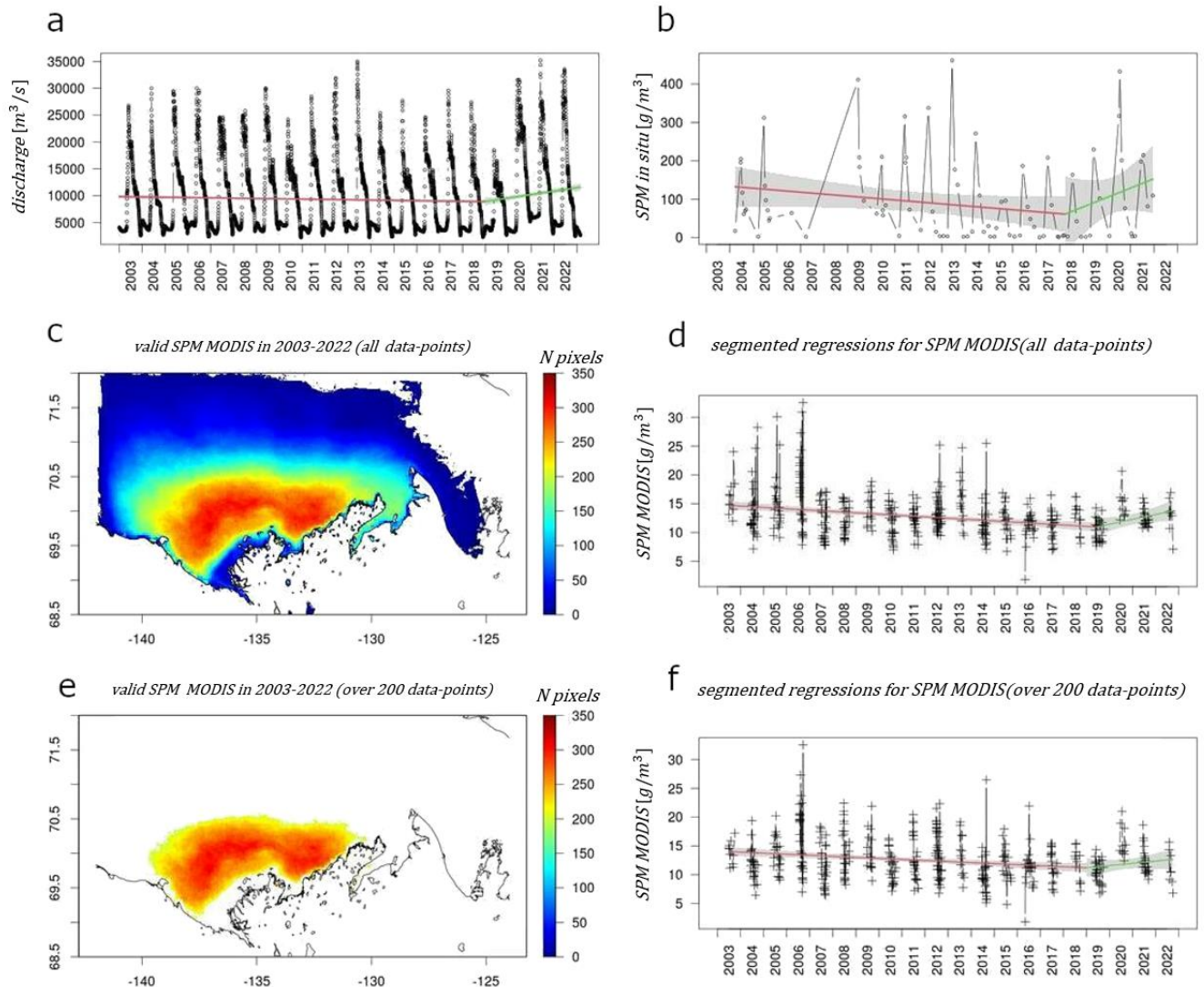


Figure 2: Interannual variations of in situ and satellite data (river discharge and SPM) with their segmented linear regression slopes (red and green colors show negative and positive regressions, respectively): (a) river discharge  $Q_{insitu}$ , (b)  $SPM_{insitu}$  time series; (c) maximum number of valid  $SPM_{sat}$  pixels in 2003-2022 (d) satellite  $SPM_{sat}$  time series; (e-f) similar to (c-d), but for the area with at least 200 valid pixels

1  
2  
3  
4 474  
5  
6 475  
7 476 **5. Data availability**  
8

9 477 In situ measurements described in section 1 (river water discharge and TSS) are  
10 478 provided at <https://arcticgreatrivers.org/data/>. MODIS data is accessible from the NASA  
11 479 website <https://oceancolor.gsfc.nasa.gov>. Sea ice concentrations are available at  
12 480 <https://seaice.uni-bremen.de/data-archive/>.  
13 481 <https://seaice.uni-bremen.de/data-archive/>.  
14 482 [ERA5 LAND reanalysis data can be found at https://doi.org/10.24381/cds.68d2bb30](https://doi.org/10.24381/cds.68d2bb30) with  
15 483 a detailed description at  
16 484 <https://confluence.ecmwf.int/display/CKB/ERA5%3A+data+documentation>, and ERA5  
17 485 wind data is available at <https://doi.org/10.24381/cds.adbb2d47> with a detailed  
18 486 description at  
19 487 [ERA5 LAND reanalysis data can be found at https://doi.org/10.24381/cds.68d2bb30](https://doi.org/10.24381/cds.68d2bb30).  
20  
21  
22  
23  
24

25 488 **6. Acknowledgments**  
26

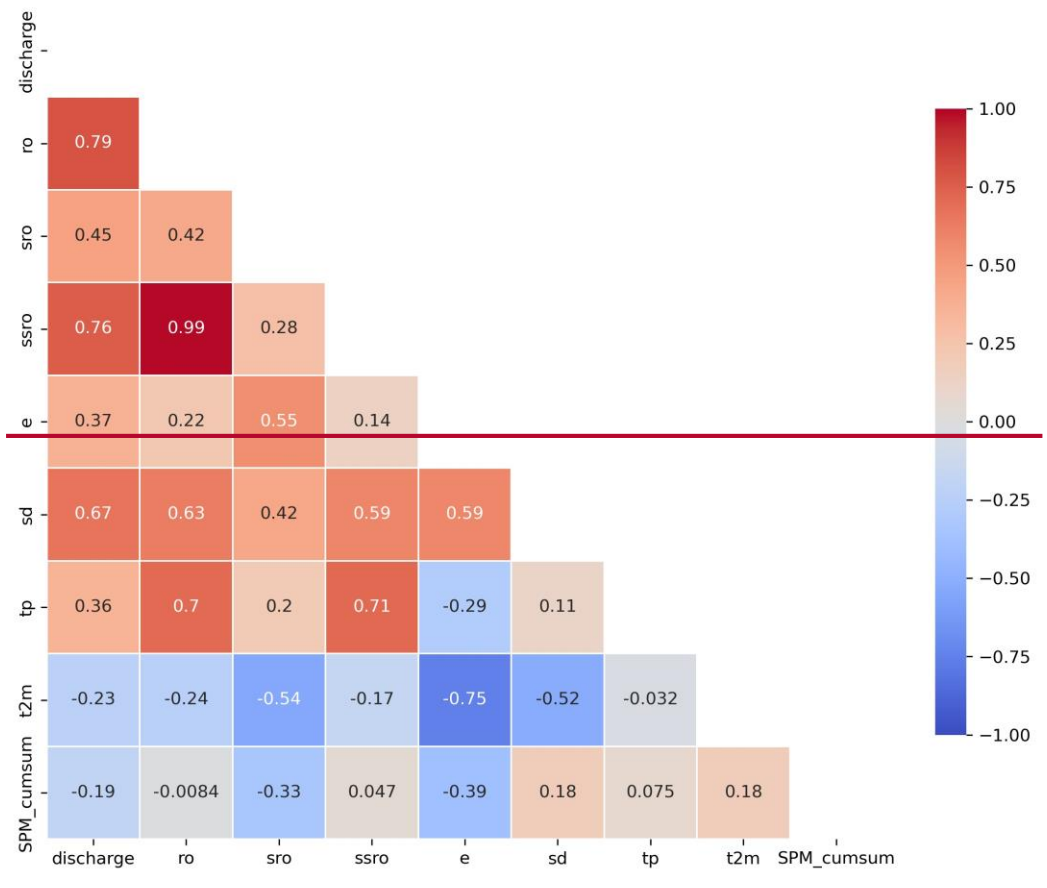
27 489 This study is part of the Nunataryuk project. The project has received funding under the  
28 490 European Union's Horizon 2020 Research and Innovation Program under grant agreement  
29 491 no. 773421. The study was co-funded by the ArcticFlux TOSCA project from the French  
30 492 space agency (CNES). The authors want also to acknowledge the NASA Goddard Space  
31 493 Flight Center, Ocean Ecology Laboratory, Ocean Biology Processing Group.  
32 494 Moderateresolution Imaging Spectroradiometer (MODIS) Aqua Data; NASA OB.DAAC,  
33 495 Greenbelt, MD, USA. doi: DOI. Accessed on 05/08/2023.  
34  
35

36 496 No conflict of interest is stated.  
37  
38

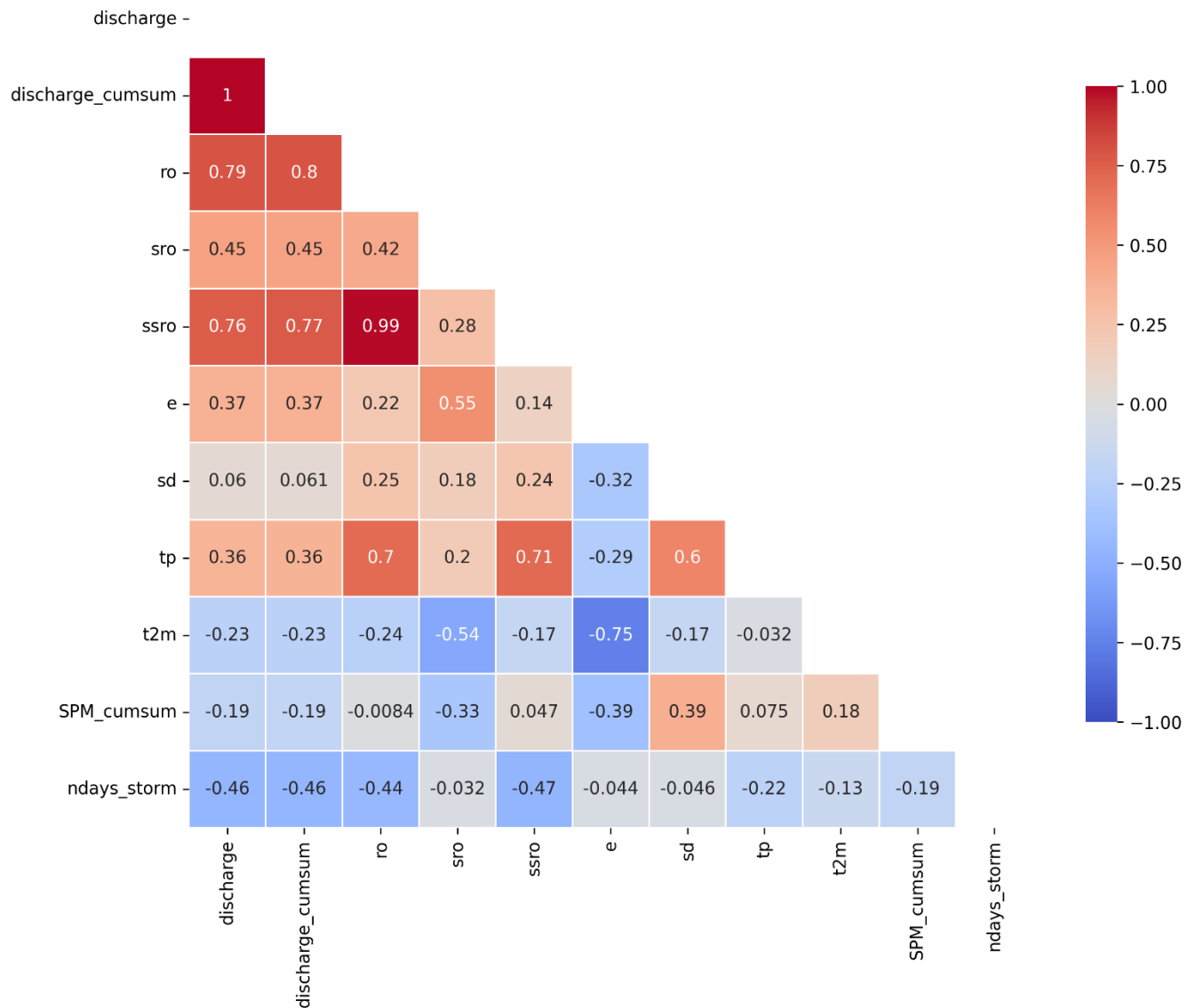
39 498 **Appendix A. ERA5-Land**  
40

41 499 The appendix contains Fig.A.3 illustrating correlation between ERA5 parameter, the  
42 500 Mackenzie discharge from the Arctic GRO dataset, and in situ and satellite SPM  
43 501 concentrations.  
44  
45  
46  
47  
48  
49  
50  
51  
52  
53  
54  
55  
56  
57  
58

1  
2  
3  
4  
5  
6  
7  
8  
9  
10  
11  
12  
13  
14  
15  
16  
17  
18  
19  
20  
21  
22  
23  
24  
25  
26  
27  
28  
29  
30  
31  
32  
33  
34  
35  
36  
37  
38  
39  
40  
41  
42  
43  
44  
45  
46  
47  
48  
49  
50  
51  
52  
53  
54  
55  
56  
57  
58  
59  
60  
61  
62  
63  
64  
65



502



503

Figure A.3: Correlation matrix of all mean yearly reanalysis (ERA5 LAND) parameters over the Mackenzie basin and in situ (Arctic GRO) discharge for Mackenzie (Arctic Red station). ERA5 Land parameters are described in main text (ro - total runoff, sro surface runoff, ssro - subsurface runoff (ssro = ro-sro), e - evaporation, sd - snow depth, tp - total precipitation, t2m - air temperature at 2 m,  $SPM_{cumsum}$  - annual cumulated SPM concentrations, discharge - Arctic GRO in situ discharge).

## References

Arias, P., Bellouin, N., Coppola, E., Jones, R., Krinner, G., Marotzke, J., Naik, V., Palmer, M., Plattner, G.K., Rogelj, J., et al., 2021. Climate Change 2021: the physical science basis. Contribution of Working Group I to the Sixth Assessment Report of the

1  
2  
3  
4  
5  
6  
7  
8  
9  
10  
11  
12  
13  
14  
15  
16  
17  
18  
19  
20  
21  
22  
23  
24  
25  
26  
27  
28  
29  
30  
31  
32  
33  
34  
35  
36  
37  
38  
39  
40  
41  
42  
43  
44  
45  
46  
47  
48  
49  
50  
51  
52  
53  
54  
55  
56  
57  
58  
59  
60  
61  
62  
63  
64  
65

513 Intergovernmental Panel on Climate Change; technical summary. Technical Report. IPCC.  
514 Geneva, Switzerland.

515 Carson, M., Jasper, J., Conly, F.M., 1998. Magnitude and sources of sediment input to the  
516 ~~mackenzie~~Mackenzie delta, northwest territories, 1974–94. *Arctic*, 116– 124.

517 Connolly, C.T., Cardenas, M.B., Burkart, G.A., Spencer, R.G., McClelland, J.W., 2020.  
518 Groundwater as a major source of dissolved organic matter to arctic coastal waters.  
519 *Nature Communications* 11, 1479.

520 DePaolo, D.J., Maher, K., Christensen, J.N., McManus, J., 2006. Sediment transport time  
521 measured with u-series isotopes: results from odp north atlantic drift site 984. *Earth and*  
522 *Planetary Science Letters* 248, 394–410.

523 Doxaran, D., Devred, E., Babin, M., 2015. A 50% increase in the mass of terrestrial particles  
524 delivered by the ~~mackenzie~~Mackenzie river into the beaufort sea (~~canadian~~Canadian  
525 arctic ocean) over the last 10 years. *Biogeosciences* 12, 3551– 3565.

526 Doxaran, D., Ehn, J., B’elanger, S., Matsuoka, A., Hooker, S., Babin, M., 2012. Optical  
527 characterisation of suspended particles in the mackenzie river plume (canadian arctic  
528 ocean) and implications for ocean colour remote sensing. *Biogeosciences* 9, 3213–3229.

529 Feng, D., Gleason, C.J., Lin, P., Yang, X., Pan, M., Ishitsuka, Y., 2021. Recent changes to arctic  
530 river discharge. *Nature communications* 12, 6917.

531 Grotheer, H., Meyer, V., Riedel, T., Pfalz, G., Mathieu, L., Hefter, J., Gentz, T., Lantuit, H.,  
532 Mollenhauer, G., Fritz, M., 2020. Burial and origin of permafrost-derived carbon in the  
533 nearshore zone of the southern canadian beaufort sea. *Geophysical Research Letters* 47,  
534 e2019GL085897.

535 Hersbach, H., Bell, B., Berrisford, P., Biavati, G., Horányi, A., Muñoz Sabater, J., Nicolas, J.,  
536 Peubey, C., Radu, R., Rozum, I., Schepers, D., Simmons, A., Soci, C., Dee, D., Thépaut, J-N.  
537 (2023): ERA5 hourly data on single levels from 1940 to present. Copernicus Climate  
538 Change Service (C3S) Climate Data Store (CDS), DOI: 10.24381/cds.adbb2d47 (Accessed  
539 on 07-SEP-2023)

540 Hilborn, A., Devred, E., 2022. Delineation of eastern beaufort sea subregions using self-  
541 organizing maps applied to 17 years of modis-aqua data. *Frontiers in Marine Science* ,  
542 1061.

543 Hill, V.J., Matrai, P.A., Olson, E., Suttles, S., Steele, M., Codispoti, L.A., Zimmerman, R.C., 2013.  
544 Synthesis of integrated primary production in the arctic ocean: Ii. in situ and remotely  
545 sensed estimates. *Progress in Oceanography* 110, 107–125.

1  
2  
3  
4  
5  
6  
7  
8  
9  
10  
11  
12  
13  
14  
15  
16  
17  
18  
19  
20  
21  
22  
23  
24  
25  
26  
27  
28  
29  
30  
31  
32  
33  
34  
35  
36  
37  
38  
39  
40  
41  
42  
43  
44  
45  
46  
47  
48  
49  
50  
51  
52  
53  
54  
55  
56  
57  
58  
59  
60  
61  
62  
63  
64  
65

Juhls, B., Matsuoka, A., Lizotte, M., B'ecu, G., Overduin, P., El Kassar, J., Devred, E., Doxaran, D., Ferland, J., Forget, M., et al., 2022. Seasonal dynamics of dissolved organic matter in the ~~mackenzie~~Mackenzie delta, ~~canadian~~Canadian arctic waters: Implications for ocean colour remote sensing. *Remote Sensing of Environment* 283, 113327.

Lizotte, M., Juhls, B., Matsuoka, A., Massicotte, P., M'evel, G., Anikina, D.O.J., Antonova, S., B'ecu, G., B'eguvin, M., B'elanger, S., et al., 2023. Nunataryuk field campaigns: Understanding the origin and fate of terrestrial organic matter in the coastal waters of the mackenzie delta region. *Earth System Science Data* 15, 1617–1653.

Massicotte, P., Amon, R.M., Antoine, D., Archambault, P., Balzano, S., B'elanger, S., Benner, R., Boeuf, D., Bricaud, A., Bruyant, F., et al., 2021. The ~~malina~~MALINA oceanographic expedition: how do changes in ice cover, permafrost and ~~uv~~UV radiation impact biodiversity and biogeochemical fluxes in the arctic ocean? *Earth System Science Data* 13, 1561–1592.

Matsuoka, A., Babin, M., Vonk, J.E., 2022. Decadal trends in the release of terrigenous organic carbon to the ~~mackenzie~~Mackenzie delta (~~canadian~~Canadian arctic) using satellite ocean color data (1998–2019). *Remote Sensing of Environment* 283, 113322.

McClelland, J., Tank, S., Spencer, R., Shiklomanov, A., Zolkos, S., Holmes, R., 2023. Arctic great rivers observatory. Data retrieved from Arctic Great Rivers Observatory. Discharge Dataset, Version 20230630. <https://www.arcticrivers.org/data>.

Miner, K.R., Turetsky, M.R., Malina, E., Bartsch, A., Tamminen, J., McGuire, A.D., Fix, A., Sweeney, C., Elder, C.D., Miller, C.E., 2022. Permafrost carbon emissions in a changing arctic. *Nature Reviews Earth and Environment* 3, 55–67.

Muggeo, V.M., 2003. Estimating regression models with unknown breakpoints. *Statistics in medicine* 22, 3055–3071.

Mun˜oz-Sabater, J., Dutra, E., Agust'ı-Panareda, A., Albergel, C., Arduini, G., Balsamo, G., Boussetta, S., Choulga, M., Harrigan, S., Hersbach, H., et al., 2021. Era5-land: A state-of-the-art global reanalysis dataset for land applications. *Earth System Science Data* 13, 4349–4383.

Mu˜noz Sabater, J. (2019): ERA5-Land monthly averaged data from 1950 to present. Copernicus Climate Change Service (C3S) Climate Data Store (CDS). DOI: 10.24381/cds.68d2bb30 (Accessed on 07-SEP-2023)

Nitze, I., Cooley, S.W., Duguay, C.R., Jones, B.M., Grosse, G., 2020. The catastrophic thermokarst lake drainage events of 2018 in northwestern ~~alaska~~Alaska: fast-forward into the future. *The Cryosphere* 14, 4279–4297.

1  
2  
3  
4  
5  
6  
7  
8  
9  
10  
11  
12  
13  
14  
15  
16  
17  
18  
19  
20  
21  
22  
23  
24  
25  
26  
27  
28  
29  
30  
31  
32  
33  
34  
35  
36  
37  
38  
39  
40  
41  
42  
43  
44  
45  
46  
47  
48  
49  
50  
51  
52  
53  
54  
55  
56  
57  
58  
59  
60  
61  
62  
63  
64  
65

Ody, A., Doxaran, D., Verney, R., Bourrin, F., Morin, G.P., Pairaud, I., Gangloff, A., 2022. Ocean color remote sensing of suspended sediments along a continuum from rivers to river plumes: Concentration, transport, fluxes and dynamics. *Remote Sensing* 14, 2026.

Poërtner, H.O., Roberts, D.C., Adams, H., Adler, C., Aldunce, P., Ali, E., Begum, R.A., Betts, R., Kerr, R.B., Biesbroek, R., et al., 2022. *Climate change 2022: Impacts, adaptation and vulnerability*. IPCC Geneva, Switzerland.

Spreen, G., Kaleschke, L., Heygster, G., 2008. Sea ice remote sensing using ~~amsr~~AMSR-e 89-ghz channels. *Journal of Geophysical Research: Oceans* 113.

Vigier, N., Bourdon, B., Turner, S., Allégre, C.J., 2001. Erosion timescales derived from u-decay series measurements in rivers. *Earth and Planetary Science Letters* 193, 549–563.

Wagner, A., Lohmann, G., Prange, M., 2011. Arctic river discharge trends since 7 ka bp. *Global and Planetary Change* 79, 48–60.

Wang, M., Shi, W., 2007. The nir-swir combined atmospheric correction approach for modis ocean color data processing. *Optics express* 15, 15722– 15733.

Webb, E.E., Liljedahl, A.K., 2023. Diminishing lake area across the northern permafrost zone. *Nature Geoscience* 16, 202–209.

Wegner, C., Hölemann, J.A., Dmitrenko, I., Kirillov, S., Kassens, H., 2005. Seasonal variations in arctic sediment dynamics—evidence from 1-year records in the Laptev sea (Siberian arctic). *Global and Planetary Change* 48, 126–140.

Winkelbauer, S., Mayer, M., Seitner, V., Zsoter, E., Zuo, H., Haimberger, L., 2022. Diagnostic evaluation of river discharge into the arctic ocean and its impact on oceanic volume transports. *Hydrology and Earth System Sciences* 26, 279–304.

Woo, M.K., Thorne, R., 2003. Streamflow in the Mackenzie basin, Canada. *Arctic*, 328–340.

Yang, D., Shi, X., Marsh, P., 2015. Variability and extreme of Mackenzie river daily discharge during 1973–2011. *Quaternary International* 380, 159–168.

Zolkos, S., Zhulidov, A.V., Gurtovaya, T.Y., Gordeev, V.V., Berdnikov, S., Pavlova, N., Kalko, E.A., Kuklina, Y.A., Zhulidov, D.A., Kosmenko, L.S., et al., 2022. Multidecadal declines in particulate mercury and sediment export from ~~russian~~Russian rivers in the pan-arctic basin. *Proceedings of the National Academy of Sciences* 119, e2119857119.

### **Declaration of interests**

The authors declare that they have no known competing financial interests or personal relationships that could have appeared to influence the work reported in this paper.

The authors declare the following financial interests/personal relationships which may be considered as potential competing interests:



AT has written the original and revised manuscript, participated in the investigation, visualization and data analysis. DD did the conceptualization, project administration, supervision and manuscript revision and editing. BG did the data curation, formal analysis, visualization and manuscript editing.